

Effective Dielectric Tensor for Electromagnetic Wave Propagation in Random Media

Mikael C. Rechtsman¹ and Salvatore Torquato^{1,2,3,4,5*}

¹*Department of Physics, Princeton University, Princeton, New Jersey, 08544*

²*Department of Chemistry, Princeton University, Princeton, New Jersey, 08544*

³*Program in Applied and Computational Mathematics, Princeton, New Jersey, 08544*

⁴*Princeton Institute for the Science and Technology
of Materials, Princeton, New Jersey, 08544 and*

⁵*Princeton Center for Theoretical Physics, Princeton, New Jersey, 08544*

(Dated: February 1, 2008)

Abstract

We derive exact strong-contrast expansions for the effective dielectric tensor ϵ_e of electromagnetic waves propagating in a two-phase composite random medium with isotropic components explicitly in terms of certain integrals over the n -point correlation functions of the medium. Our focus is the long-wavelength regime, i.e., when the wavelength is much larger than the scale of inhomogeneities in the medium. Lower-order truncations of these expansions lead to approximations for the effective dielectric constant that depend upon whether the medium is below or above the percolation threshold. In particular, we apply two- and three-point approximations for ϵ_e to a variety of different three-dimensional model microstructures, including dispersions of hard spheres, hard oriented spheroids and fully penetrable spheres as well as Debye random media, the random checkerboard, and power-law-correlated materials. We demonstrate the importance of employing n -point correlation functions of order higher than two for high dielectric-phase-contrast ratio. We show that disorder in the microstructure results in an imaginary component of the effective dielectric tensor that is directly related to the *coarseness* of the composite, i.e., local volume-fraction fluctuations for infinitely large windows. The source of this imaginary component is the attenuation of the coherent homogenized wave due to scattering. We also remark on whether there is such attenuation in the case of a two-phase medium with a quasiperiodic structure.

PACS numbers: 05.40.-a, 41.20.Jb, 77.22.Ch

*Electronic address: torquato@electron.princeton.edu

I. INTRODUCTION

The problem of determining the effective dielectric tensor and other mathematically equivalent properties of random media dates back to the classic work of Maxwell [1]. Calculation of the effective dielectric tensor of disordered composite materials is essential for a wide range of applications, including remote sensing (e.g., of terrain, vegetation, etc.) [2], the study of wave propagation through turbulent atmospheres [3], active manipulation of composites [4], and as a probe of artificial materials [5]. The effective dielectric tensor at long wavelengths plays a particularly important role in the study of electrostatic resonances [6, 7].

This paper is concerned with the calculation of the effective dielectric tensor ϵ_e of a two-phase dielectric random medium associated with electromagnetic wave propagation in the long wavelength regime, i.e., when the wavelength is much larger than the scale of inhomogeneities in the medium. The complementary regime, in which the wavelength is much smaller than the inhomogeneities, may be studied numerically using a ray-tracing technique based on geometrical optics [8]. The purely static (as opposed to the full dynamic) problem, on which Maxwell's work was centered, can be considered to be a special case of the present work in the limit of infinite wavelength (or zero frequency). Although there has been extensive previous work on the dynamic problem (see Refs. 9 and 10 and references therein), the vast majority of studies that attempt to relate ϵ_e to the microstructure employ only two-point correlation information [5, 11, 12] (with a few exceptions, see, e.g., Ref. 13). On the other hand, there has been a great deal of work on the static problem incorporating three-point and higher-order correlation functions; see, for example Refs. 14, 15, 16, 17, 18, 19, and references therein.

Here we present, for the first time, explicit closed-form series expansions for the effective dielectric tensor of two-phase random media in three dimensions in terms of certain integrals of n -point correlation functions for the dynamic problem in the long-wavelength regime. The approach used follows directly from one given originally for the purely static problem in any dimension in Ref. 17, and expanded upon in Ref. 19. An advantageous feature of this formalism is that it gives rise to expansion parameters involving the dielectric constants that yield very good convergence properties even for high phase-contrast ratio. The technique is called the *strong-contrast expansion* for this reason. Tsang and Kong [11] have employed

a similar method, but only up to the two-point level and they provide no justification for or limitations on the class of microstructures and phase-contrast ratios for which their two-point approximation is applicable. We restrict ourselves to considering component materials that are themselves isotropic but that generally possess complex-valued dielectric constants. As we will demonstrate, lower-order truncated forms of these expansions can serve as useful approximations of the effective dielectric tensor. Although the formalism is applied here to electromagnetism in three dimensions, it is straightforwardly generalizable to a class of other vector fields in arbitrary dimension [19].

We obtain new approximations for ϵ_e by truncating the exact strong-contrast expansions at the two-point and three-point levels that depend upon whether the medium is below or above its percolation threshold. Using these two-point approximations, we estimate ϵ_e of dispersions of hard spheres, hard oriented spheroids and fully penetrable spheres as well as Debye random media, random checkerboard, and power-law-correlated materials. We use a three-point approximation to evaluate the effective dielectric constant in the case of the fully-penetrable-sphere model in order to establish the importance of three-point information at high phase-contrast ratio and volume fraction, and assess the accuracy of the two-point approximations. For many of the model microstructure considered here, the explicit forms of the corresponding n -point correlation functions follow from the general representation formalism of Torquato and Stell [20].

A significant qualitative difference between the purely static problem and the dynamic problem is that in the latter, the effective dielectric tensor may be complex even if the component materials have purely real dielectric constants. This results from incoherent scattering of the incident wave. The imaginary component of the effective dielectric tensor has special significance to remote sensing applications, as it plays a key role in, for example, the calculation of backscattering coefficients [11]. Although the expansions we derive here are applicable in general to materials with complex dielectric constants, we will apply them to cases in which the material phases have real dielectric constants. We do this because in this regime, disordered media will in general yield nonnegative imaginary contributions to the effective dielectric tensor purely due to scattering, not absorption. The physical manifestation of this can be understood in the context of optical or ultrasonic transmission experiments [21, 22], in which a wave pulse propagates through a finite-sized slab composed of a disordered material, and the transmitted signal is measured. The transmitted field

is observed to be a superposition of a coherent pulse representing the incident signal and uncorrelated noise due to random scattering. The attenuation of the incident pulse is a consequence of this scattering. Since periodic media propagate waves without any loss (and thus with purely real effective dielectric tensors), they do not exhibit imaginary parts in their effective dielectric tensors. In the case of statistically homogeneous and isotropic media in particular, we show here that the leading-order contribution to the imaginary component of the effective dielectric constant is directly related to the *coarseness* C_∞ of the composite for an infinitely large window. The coarseness is defined as the standard deviation of the volume fraction of a given phase, in some observation “window” within the composite divided by the total volume fraction of that phase [19, 23]. It has recently been suggested that local density fluctuations provides a crude measure of disorder of a system [24, 25]. In the language of Ref. 24, a *hyperuniform* system is one in which $C_\infty = 0$, which has been shown to always be the case for periodic systems, and therefore is consistent with the fact that $\text{Im}[\epsilon_e] = 0$ for such media. Note that a non-zero imaginary component of the effective dielectric constant can be directly associated with a mean free path of waves propagating through the given medium [10].

In Section II, we introduce our formalism, derive the strong-contrast expansion for the effective dielectric tensor, and discuss the approach towards applying these techniques at the three-point level. In Section III, we discuss a variety of model microstructures not previously studied in the present context and their associated two-point correlation functions. In Section IV, we present results for the model microstructures discussed in Section III, showing volume fraction and dielectric-contrast ratio dependence at the two-point level, and demonstrating the importance of three-point calculations at sufficiently high phase contrasts and volume fractions. In Section V, we discuss conclusions based on our results. Appendix A presents a generalization of our formalism, up to the two-point level, wherein the expansion is carried out with an arbitrary “reference” or “comparison” material (as described in Section II.A). discussed hence). Appendix B gives a short proof of why periodic media, at low frequencies, must give rise to effective dielectric tensors with no imaginary component. Finally, in Appendix C, we simplify the key two-point integral for statistically homogeneous but anisotropic media with azimuthal symmetry, an example of which is a dispersion of hard oriented spheroids.

II. THEORY

Here we extend the formalism for determining strong-contrast expansions of the purely static effective dielectric tensor in arbitrary space dimensions [17, 19] to the dynamic case in \mathbb{R}^3 when the wavelength is much larger than the inhomogeneity length scale. This method is based on finding solutions of certain integral equations using the method of Green's functions.

A. Strong-Contrast Expansions

Following Ref. 19 (which gives greater detail than Ref. [17]), we begin by considering a macroscopically large ellipsoidal sample composite material in \mathbb{R}^3 composed of two phases, labeled 1 and 2, which is itself embedded in a homogeneous “reference” (or “comparison”) material of dielectric constant ε_0 . We choose a specific macroscopic shape to call attention to the fact that the average fields in the problem are shape dependent. An advantage of this formalism is that it eliminates the shape dependence of the effective dielectric tensor. The length scale of inhomogeneities within the composite is assumed to be much smaller than the shape itself. The two phases have dielectric constants ε_1 and ε_2 , and we define indicator functions in the following way:

$$\mathcal{I}^{(p)}(\mathbf{r}) = \begin{cases} 1, & \text{if } \mathbf{r} \text{ lies in phase } p \\ 0, & \text{otherwise} \end{cases} \quad (1)$$

for $p = 1, 2$. Thus, the volume fractions of the phases are $\langle \mathcal{I}^{(p)}(\mathbf{r}) \rangle = \phi_p$ and $\phi_q = 1 - \phi_p$ ($p \neq q$). We may therefore write $\varepsilon(\mathbf{r}) = \varepsilon_1 \mathcal{I}^{(1)}(\mathbf{r}) + \varepsilon_2 \mathcal{I}^{(2)}(\mathbf{r})$ in the composite. Note that the dielectric constants ε_1 and ε_2 may be complex.

When solved for the electric field, time-harmonic Maxwell's equations reduce to

$$\nabla \times \nabla \times \mathbf{E}(\mathbf{r}) - \varepsilon(\mathbf{r}) \left(\frac{\omega}{c} \right)^2 \mathbf{E}(\mathbf{r}) = 0, \quad (2)$$

with \mathbf{E} the electric field, $\varepsilon(\mathbf{r})$ the reduced dielectric constant, ω the frequency of the time-harmonic solution, and c the speed of light. We assume here that $\mu/\mu_0 = 1$, and that the component dielectric materials are themselves isotropic. We can rewrite this homogeneous, linear equation in a form that is suggestive of perturbation theory:

$$\nabla \times \nabla \times \mathbf{E}(\mathbf{r}) - \varepsilon_q \left(\frac{\omega}{c} \right)^2 \mathbf{E}(\mathbf{r}) = (\varepsilon(\mathbf{r}) - \varepsilon_q) \left(\frac{\omega}{c} \right)^2 \mathbf{E}(\mathbf{r}), \quad (3)$$

where we have taken the comparison material to be one of the phase materials, i.e., $\varepsilon_0 = \varepsilon_q$, where q is either 1 or 2. We employ this choice for simplicity here, but this is not essential; in fact, depending on the details of the structure in question, it may improve convergence to choose a different comparison material [19, 26, 27]. We discuss this point in further detail in Appendix A.

As a shorthand, we will define $k_q^2 \equiv \sigma_q \equiv \left(\frac{\omega}{c}\right)^2 \varepsilon_q$, for any phase, $q = 1$ or 2 . In order to solve this equation for an arbitrary structure via perturbation theory, we require a Green's function for the operator on the left side of Eq. (3), which must therefore be a tensor. This is the dyadic Green's function. In three-dimensional spherical coordinates, it is given by

$$\mathbf{G}(\mathbf{r}, \mathbf{r}') = -\frac{\mathbf{I}}{d\sigma_q} \delta(\mathbf{r} - \mathbf{r}') + G_1(\mathbf{r} - \mathbf{r}')\mathbf{I} + G_2(\mathbf{r} - \mathbf{r}')\hat{\mathbf{r}}\hat{\mathbf{r}}, \quad (4)$$

where

$$\begin{aligned} G_1(\mathbf{r} - \mathbf{r}') &= (-1 + ik_q r + k_q^2 r^2) \frac{e^{ik_q r}}{4\pi k_q^2 r^3}, \\ G_2(\mathbf{r} - \mathbf{r}') &= (3 - 3ik_q r - \sigma_q r^2) \frac{e^{ik_q r}}{4\pi k_q^2 r^3}, \end{aligned}$$

with $r = |\mathbf{r} - \mathbf{r}'|$, $\hat{\mathbf{r}}$ is a unit vector directed from \mathbf{r}' towards \mathbf{r} , and \mathbf{I} is the unit tensor in three dimensions. In the limit $k_q \rightarrow 0$, we recover the static result [19] in three dimensions. Note the delta function in this expression; this is the dipole “source” of the radiation; its coefficient is dependent on the shape of the “exclusion volume” around this source. For the coefficient shown, the exclusion volume must be spherical in shape.

The Green's function satisfies the following partial differential equation:

$$\nabla \times \nabla \times \mathbf{G}(\mathbf{r}, \mathbf{r}') - \sigma_q \mathbf{G}(\mathbf{r}, \mathbf{r}') = \mathbf{I} \delta(\mathbf{r} - \mathbf{r}'). \quad (5)$$

This implies that we can write the electric field as

$$\mathbf{E}(\mathbf{r}) = \mathbf{E}_0(\mathbf{r}) + \int d\mathbf{r}' \mathbf{G}(\mathbf{r}, \mathbf{r}') [\sigma(\mathbf{r}) - \sigma_q] \mathbf{E}(\mathbf{r}'). \quad (6)$$

We can express this integral equation more compactly in linear operator form:

$$\mathbf{E} = \mathbf{E}_0 + \mathbf{G}\mathbf{P}, \quad (7)$$

where we define the polarization vector field as

$$\mathbf{P} = [\sigma(\mathbf{r}) - \sigma_q] \mathbf{E}. \quad (8)$$

The next step is to extract the delta function contribution from the Green's function solution. In doing so, we obtain a new field, \mathbf{F} , the *cavity intensity field*, which is directly proportional to \mathbf{E} . The resulting integral equation is

$$\mathbf{F} = \mathbf{E}_0 + \mathbf{H}\mathbf{P}, \quad (9)$$

where \mathbf{H} is the principle value of the Green's function in Eq. (4), namely

$$\mathbf{H}(\mathbf{r} - \mathbf{r}') = G_1(\mathbf{r} - \mathbf{r}')\mathbf{I} + G_2(\mathbf{r} - \mathbf{r}')\hat{\mathbf{r}}\hat{\mathbf{r}}. \quad (10)$$

Here, we have defined

$$\mathbf{F}(\mathbf{r}) = \left[\mathbf{I} + \frac{\sigma(\mathbf{r}) - \sigma_q}{d\sigma_q} \right] \cdot \mathbf{E}(\mathbf{r}), \quad (11)$$

where \mathbf{I} is the unit dyadic tensor. Now, \mathbf{P} and \mathbf{F} are directly related:

$$\mathbf{P}(\mathbf{r}) = \frac{\sigma(\mathbf{r}) - \sigma_q}{\mathbf{I} + \frac{\mathbf{I}}{d\sigma_q} [\sigma(\mathbf{r}) - \sigma_q]} \mathbf{F}(\mathbf{r}). \quad (12)$$

or, implicitly defining \mathbf{L} ,

$$\mathbf{P}(\mathbf{r}) = \mathbf{L}(\mathbf{r}) \cdot \mathbf{F}(\mathbf{r}). \quad (13)$$

Note that \mathbf{L} is an isotropic tensor. Instead of using the standard definition of the effective dielectric tensor, $\langle \mathbf{D} \rangle = \varepsilon_e \cdot \langle \mathbf{E} \rangle$, we may equally well use the above equation. Thus, implicitly defining \mathbf{L}_e , we have

$$\langle \mathbf{P}(\mathbf{r}) \rangle = \mathbf{L}_e \cdot \langle \mathbf{F}(\mathbf{r}) \rangle, \quad (14)$$

where $\langle . \rangle$ denotes the ensemble (volume) average (assuming ergodicity). We may write \mathbf{L}_e explicitly at this point. It is given by

$$\mathbf{L}_e = L_e \mathbf{I} = \frac{\sigma_e - \sigma_q}{\mathbf{I} + \frac{\mathbf{I}}{d\sigma_q} [\sigma_e - \sigma_q]}, \quad (15)$$

where $\sigma_e = \left(\frac{\omega}{c}\right)^2 \varepsilon_e$, with ε_e the effective dielectric tensor of the composite.

We now have an equation that defines the effective dielectric tensor. The last step involves eliminating the background field, \mathbf{E}_0 . This is done because, as is known from electrostatics, the relationship between the applied field and the average fields (\mathbf{P} and \mathbf{L} , for example) is shape-dependent. Thus, eliminating \mathbf{E}_0 results in an effective dielectric constant that is independent of the shape of the macroscopic ellipsoid. It has been demonstrated that the

elimination \mathbf{E}_0 thus leads to integrals of correlation functions within the formalism that are absolutely convergent [17, 19].

We define here a new tensor operator \mathbf{S} in the following way:

$$\mathbf{S} = \mathbf{L} [\mathbf{I} - \mathbf{LH}]^{-1}. \quad (16)$$

It follows directly that $\langle \mathbf{P} \rangle = \langle \mathbf{S} \rangle \mathbf{E}_0$, and we may thus eliminate \mathbf{E}_0 from Eq. (9). Upon taking the ensemble average of the latter, we may write $\langle \mathbf{F} \rangle$ in terms of $\langle \mathbf{P} \rangle$, the first few terms of which are given by:

$$\langle \mathbf{F}(\mathbf{r}_1) \rangle = \frac{\langle \mathbf{P}(\mathbf{r}_1) \rangle}{\langle L(\mathbf{r}_1) \rangle} - \int d\mathbf{r}_2 \left[\frac{\langle L(\mathbf{r}_1)L(\mathbf{r}_2) \rangle - \langle L(\mathbf{r}_1) \rangle \langle L(\mathbf{r}_2) \rangle}{\langle L(\mathbf{r}_1) \rangle \langle L(\mathbf{r}_2) \rangle} \right] \mathbf{H}(\mathbf{r}_1, \mathbf{r}_2) \langle \mathbf{P}(\mathbf{r}_2) \rangle - \quad (17)$$

$$\int d\mathbf{r}_2 d\mathbf{r}_3 \left[\frac{\langle L(\mathbf{r}_1)L(\mathbf{r}_2)L(\mathbf{r}_3) \rangle}{\langle L(\mathbf{r}_1) \rangle \langle L(\mathbf{r}_2) \rangle} - \frac{\langle L(\mathbf{r}_1)L(\mathbf{r}_2) \rangle \langle L(\mathbf{r}_2)L(\mathbf{r}_3) \rangle}{\langle L(\mathbf{r}_1) \rangle \langle L(\mathbf{r}_2) \rangle \langle L(\mathbf{r}_3) \rangle} \right] \mathbf{H}(\mathbf{r}_1, \mathbf{r}_2) \mathbf{H}(\mathbf{r}_2, \mathbf{r}_3) \langle \mathbf{P}(\mathbf{r}_3) \rangle - \dots \quad (18)$$

From this expression and Eq. (14), we obtain the following exact expansions for statistically homogeneous media involving the effective dielectric tensor:

$$\beta_{pq}^2 \phi_p^2 (\sigma_e - \sigma_q \mathbf{I})^{-1} (\sigma_e + 2\sigma_q \mathbf{I}) = \phi_p \beta_{pq} \mathbf{I} - \sum_{n=2}^{\infty} \mathbf{A}_n^{(p)} \beta_{pq}^n, \quad (p \neq q), \quad (19)$$

where $p \neq q$,

$$\beta_{pq} = \frac{\sigma_p - \sigma_q}{\sigma_p + (d-1)\sigma_q} = \frac{\varepsilon_p - \varepsilon_q}{\varepsilon_p + (d-1)\varepsilon_q}, \quad (20)$$

and the n -point tensor coefficients $\mathbf{A}_n^{(p)}$ are certain integrals over the n -point correlation functions $S_n^{(p)}$ associated with phase p . In particular, for $n = 2$

$$\mathbf{A}_2^{(p)} = \frac{d}{\Omega} \int d\mathbf{r} \mathbf{t}^{(p)}(\mathbf{r}) \left[S_2^{(p)}(\mathbf{r}) - \phi_p^2 \right], \quad (21)$$

where

$$\mathbf{t}^{(p)}(\mathbf{r}) = \Omega k_q^2 \mathbf{H}(\mathbf{r}), \quad (22)$$

and Ω is the solid angle of a sphere in dimension d , and $\mathbf{H}(\mathbf{r})$ is given by Eq. (10). For any $n > 2$, we have

$$\mathbf{A}_n^{(p)} = \left(\frac{-1}{\phi_p} \right)^{n-2} \left(\frac{d}{\Omega} \right)^{n-1} \int d\mathbf{r}_2 \dots \int d\mathbf{r}_n \mathbf{t}^{(p)}(\mathbf{r}_1, \mathbf{r}_2) \cdot \mathbf{t}^{(p)}(\mathbf{r}_2, \mathbf{r}_3) \dots \mathbf{t}^{(p)}(\mathbf{r}_{n-1}, \mathbf{r}_n) \Delta_n^{(p)}(\mathbf{r}_1, \dots, \mathbf{r}_n), \quad (23)$$

where $\Delta_n^{(p)}(\mathbf{r}_1, \dots, \mathbf{r}_n)$ the determinant is given by

$$\Delta_n^{(p)} = \begin{vmatrix} S_2^{(p)}(\mathbf{r}_1, \mathbf{r}_2) & S_1^{(p)}(\mathbf{r}_2) & \cdots & 0 \\ S_3^{(p)}(\mathbf{r}_1, \mathbf{r}_2, \mathbf{r}_3) & S_2^{(p)}(\mathbf{r}_2, \mathbf{r}_3) & \cdots & 0 \\ \vdots & \vdots & \ddots & \vdots \\ S_n^{(p)}(\mathbf{r}_1, \dots, \mathbf{r}_n) & S_{n-1}^{(p)}(\mathbf{r}_2, \dots, \mathbf{r}_n) & \cdots & S_2^{(p)}(\mathbf{r}_{n-1}, \mathbf{r}_n) \end{vmatrix} \quad (24)$$

and

$$S_n^{(p)}(\mathbf{r}_1, \mathbf{r}_2, \dots, \mathbf{r}_n) \equiv \langle I^{(p)}(\mathbf{r}_1) I^{(p)}(\mathbf{r}_2) \cdots I^{(p)}(\mathbf{r}_n) \rangle. \quad (25)$$

is the n -point correlation function of phase p . For statistically homogeneous media (the case for which this formulation applies), the latter quantity is translationally invariant and therefore depends only on relative displacements, i.e., $S_n^{(p)}(\mathbf{r}_1, \mathbf{r}_2, \dots, \mathbf{r}_n) = S_n^{(p)}(\mathbf{r}_{12}, \mathbf{r}_{13}, \dots, \mathbf{r}_{1n})$, where we have chosen point 1 to be the origin, and, in particular, $S_1^{(p)}(\mathbf{r}_1) = \phi_p$.

Remarks

1. We see that the integral-equation approach given here is entirely general. It is equally well suited to any problem in which the local and averaged constitutive relations have the same form, and thus the appropriate dyadic Green's function would replace Eq. (4). Indeed, the determinant (24) for the dynamic problem considered here is exactly the same as that in the static problem, as given originally in Ref. 17.
2. Note that Eq. (19) represents two different series expansions: one for $q = 1$ and $p = 2$ and the other for $q = 2$ and $p = 1$.
3. The quantity β_{pq} , given in Eq. (20), is the strong-contrast expansion parameter, the form of which is a direct consequence of the choice of exclusion volume associated with the source-term of the Green's function. Any shape besides the sphere would have necessarily led to a different expansion parameter and therefore to significantly different convergence properties [19]. Clearly, β_{pq} may lie within the range $-(d-1)^{-1} \leq \beta_{pq} \leq 1$. The radius of convergence of the series given in Eq. (19) is thus greatly widened beyond that of a weak-contrast expansion (i.e., the simple difference of the phase dielectric constants).
4. In the purely static case, the series represented by (19) may be regarded as expansions that perturb around the optimal structures that realize the generalized Hashin-Shtrikman bounds [28] derived by Willis [29], as discussed by Torquato [19]. In particular, these optimal structures are certain dispersions in which there is a disconnected, dispersed phase in a

connected matrix phase. The lower bound corresponds to the case when the high-dielectric-constant phase is the dispersed, disconnected phase and the upper bound corresponds to the instance in which the high-dielectric constant phase is the connected matrix. Thus, we expect that for the dynamic problem under consideration, the first few terms of the expansion (19) with $q = 1$ and $p = 2$ will yield a reasonable approximation of ε_e for two-phase media, depending on whether the high-dielectric phase is below or above its percolation threshold, as discussed further in Section II.C.

B. Macroscopically Isotropic Media

Consider, as we will to a large extent in this paper, two-phase media that are statistically homogeneous and isotropic, and thus macroscopically isotropic. In this case, the effective dielectric tensor is proportional to the identity tensor, and can thus be treated as a simple scalar, namely, the effective dielectric constant of the medium. This of course simplifies the calculation enormously. We thus take the trace of both sides of Eq. (19) and divide by d . Thus, the full expression in the isotropic case is given by

$$\beta_{pq}^2 \phi_p^2 \beta_{eq}^{-1} = \phi_p \beta_{pq} - \sum_{n=2}^{\infty} A_n^{(p)} \beta_{pq}^n, \quad (26)$$

where $A_n^{(p)} = \text{Tr} [\mathbf{A}_n^{(p)}] / d$ and β_{eq} is the effective polarizability, given by

$$\beta_{eq} = \frac{\varepsilon_e - \varepsilon_q}{\varepsilon_p + (d-1)\varepsilon_q}. \quad (27)$$

The scalar two-point coefficient, as specified by taking the trace of (21), is given by

$$A_2^{(p)} = \frac{d}{\Omega} \int d\mathbf{r} \frac{\text{Tr} [\mathbf{t}^{(p)}(\mathbf{r})]}{d} [S_2^{(p)}(\mathbf{r}) - \phi_p^2] = 2k_q^2 \int_0^{\infty} dr \exp(ik_q r) r [S_2^{(p)}(r) - \phi_p^2], \quad (28)$$

with this integral being straightforwardly carried out either numerically or analytically, depending on the form of the correlation function. Provided that the correlation function $S_2^{(p)}(r)$ decay sufficiently rapidly to its long-range value of ϕ_p^2 , the integral in (28) will be convergent.

Note that by Eq. (28), $A_2^{(p)}$ must be zero in the purely static problem ($\omega = 0$) if the medium is statistically homogeneous and isotropic. Thus, in the static problem, assuming statistical homogeneity and isotropy, two-point information is actually incorporated even

though $A_2^{(p)}$ is zero. This subtle point is elaborated in Ref. 19. This suggests that our formalism is extremely well suited to the non-static problem in the low frequency limit being considered here. Expanding the two-point coefficient $A_2^{(p)}$ given in Eq. (28) through third order in k_q about $k_q = 0$ yields

$$A_2^{(p)} = 2k_q^2 \int_0^\infty dr r \left[S_2^{(p)}(r) - \phi_p^2 \right] + 2ik_q^3 \int_0^\infty dr r^2 \left[S_2^{(p)}(r) - \phi_p^2 \right] + \mathcal{O}(k_q^4). \quad (29)$$

It should be expected that the imaginary component of the effective dielectric constant of statistically homogeneous and isotropic systems should be positive; otherwise the homogenized coherent wave would be amplified rather than attenuated. A simple analysis of Eq. (29) bears this out. The second term on the right hand side, i.e., the leading-order imaginary component, is nothing more than the zero-wave-vector structure factor of the composite material. Since $S_2^{(p)}(r)$ is obtained from a realizable configuration, this is necessarily positive [30]. This is true because the structure factor is nothing but the squared norm of the Fourier transform of the function $\mathcal{I}^{(p)}(\mathbf{r}) - \phi_p$. The leading-order term of the imaginary component in the expansion given in Eq. (29) is directly proportional to the volume integral of the function $S_2^{(p)}(r) - \phi_p^2$. This is exactly $(\phi_2 C_\infty)^2 v_0$, where C_∞ is the coarseness of the composite structure in the limit of an infinitely large window, and v_0 is the window volume [19, 23]. Thus, the value of the nonnegative imaginary part of the effective dielectric constant to leading order is determined by local-volume-fraction fluctuation over very large windows, which may be taken to be a crude measure of disorder in the system. [24] Note also that C_∞ is proportional to the single-scattering intensity of scattered radiation from the random medium in the infinite-wavelength limit [19, 31].

Another important fact that emerges from this formalism is that at the two-point level the correction to the static effective dielectric constant only enters at second order in k_q (i.e., second order in the frequency). It is hence a relatively small contribution. The imaginary term enters only at third order in the wave number.

Now, let us consider the simplification of the three-point coefficient $A_3^{(p)}$. From the general expression (23), we find

$$A_3^{(p)} = \frac{9}{(4\pi)^2} \int d^3\mathbf{r}_{12} \int d^3\mathbf{r}_{13} \mathbf{t}^{(p)}(\mathbf{r}_{12}) \cdot \mathbf{t}^{(p)}(\mathbf{r}_{13}) \left[S_3^{(p)}(\mathbf{r}_{12}, \mathbf{r}_{13}) - \frac{S_2^{(p)}(\mathbf{r}_{12}) S_2^{(p)}(\mathbf{r}_{13})}{\phi_p} \right] \quad (30)$$

The first few terms of the Taylor expansion of (30) about $k_q = 0$ is given by

$$\begin{aligned} A_3^{(p)} &= \frac{18}{(4\pi)^2} \int \frac{d^3\mathbf{r}_{12}}{r_{12}^3} \int \frac{d^3\mathbf{r}_{13}}{r_{13}^3} \left[1 + \frac{k_q^2}{6}(r_{12}^2 + r_{13}^2) \right] P_2(\mu) \left[S_3^{(p)}(\mathbf{r}_{12}, \mathbf{r}_{13}) - \frac{S_2^{(p)}(\mathbf{r}_{12})S_2^{(p)}(\mathbf{r}_{13})}{\phi_p} \right] + \mathcal{O}(k_q^4) \\ &= 9 \int_0^\infty \frac{dr}{r} \int_0^\infty \frac{ds}{s} \int_{-1}^1 d\mu \left[1 + \frac{k_q^2}{6}(r^2 + s^2) \right] P_2(\mu) \left[S_3^{(p)}(r, s, \mu) - \frac{S_2^{(p)}(r)S_2^{(p)}(s)}{\phi_p} \right] + \mathcal{O}(k_q^4). \end{aligned} \quad (31)$$

where $\mu = \cos \theta$, θ is the angle between \mathbf{r}_{12} and \mathbf{r}_{13} and P_2 is the second-order Legendre polynomial. The simplified second line is obtained by exploiting the homogeneity and isotropy of the medium, reducing the original six-dimensional integral to a three-dimensional one [18]. Here $r = |\mathbf{r}_{12}|$ and $s = |\mathbf{r}_{13}|$ are the side lengths of a triangle and θ is the angle between these sides. Note that the third-order term in k_q is exactly zero, the next-lowest-order contribution to the real component must be of the order of k_q^4 (or higher), and the next-lowest-order contribution to the imaginary component must be of the order of k_q^5 (or higher).

In Section IV of this paper, estimates for the effective dielectric constant that include three-point information will be presented for the fully-penetrable-sphere model.

C. Two- and Three-Point Approximations

Practically speaking, it is difficult to ascertain four-point and higher-order correlation functions which therefore prohibits an exact evaluation of the expansion for the effective dielectric tensor in Eq. (19). However, as shown in the static problem [17, 19], lower-order truncations of the exact expansion (19) at the two-point and three-point levels have proved to be accurate approximations for the effective dielectric tensor. For the macroscopically isotropic case, the two-point and three-point approximations used to calculate the effective dielectric constant, obtained by truncating the series in Eq. (26), are given by

$$\left[\frac{\varepsilon_p - \varepsilon_q}{\varepsilon_p + (d-1)\varepsilon_q} \right] \phi_p^2 \left[\frac{\varepsilon_e - \varepsilon_q}{\varepsilon_e + (d-1)\varepsilon_q} \right]^{-1} = \phi_p - A_2^{(p)} \left[\frac{\varepsilon_p - \varepsilon_q}{\varepsilon_p + (d-1)\varepsilon_q} \right], \quad (p \neq q), \quad (32)$$

and

$$\left[\frac{\varepsilon_p - \varepsilon_q}{\varepsilon_p + (d-1)\varepsilon_q} \right] \phi_p^2 \left[\frac{\varepsilon_e - \varepsilon_q}{\varepsilon_e + (d-1)\varepsilon_q} \right]^{-1} = \phi_p - A_2^{(p)} \left[\frac{\varepsilon_p - \varepsilon_q}{\varepsilon_p + (d-1)\varepsilon_q} \right] - A_3^{(p)} \left[\frac{\varepsilon_p - \varepsilon_q}{\varepsilon_p + (d-1)\varepsilon_q} \right]^2, \quad (p \neq q), \quad (33)$$

respectively, where $A_2^{(p)}$ is given by Eq. (29), and $A_3^{(p)}$ is given by Eq. (31). The two-point approximation (32) is exact to second order in $\varepsilon_p - \varepsilon_q$ for any ϕ_p and is exact to first order in

ϕ_p for any phase-contrast ratio $\varepsilon_p/\varepsilon_q$. The three-point approximation (33) is exact to third order in $\varepsilon_p - \varepsilon_q$ for any ϕ_p and is exact to first order in ϕ_p for any phase-contrast ratio $\varepsilon_p/\varepsilon_q$. However, the most difficult cases to treat theoretically are when both the volume fraction and phase-contrast ratio are significantly different from zero and unity, respectively. The strong-contrast approximations (32) and (33) are expected to provide reasonable estimates of ε_e for a certain class of dispersions in this more difficult regime because they are perturbations of the strong-contrast expansions in the infinite-wavelength limit (pure static case), which have been shown to be in excellent agreement with both precise computer-simulation and experimental data for a variety of dispersions [17, 19]. Specifically, if $\epsilon_p > \epsilon_q$, (32) and (33) with $q = 1$ and $p = 2$ will yield good estimates of ε_e provided that phase 2 is below its percolation threshold and that the typical cluster size of phase 2 is sufficiently small [17, 19]. On the other hand, if phase 2 is above its percolation threshold, (32) and (33) with $q = 2$ and $p = 1$ should provide good estimates of ε_e .

III. MODEL MICROSTRUCTURES

We study a number of model microstructures and their corresponding two-point correlation functions. In particular, we examine dispersions of hard spheres, hard oriented spheroids and fully penetrable spheres as well as Debye random media, the random checkerboard, and power-law-correlated materials. Except for the hard-ellipsoid model, all of the other models are statistically homogeneous and isotropic. We take a to be a characteristic length scale for each model. These microstructures, depicted in Fig. 1 are explicitly described in this section, and we take $q = 1$ and $p = 2$. The two-point correlation functions for each of these models is depicted in Fig. 2, at volume fraction $\phi_2 = 0.5$, with correlation lengths roughly equal to one another. The “correlation length” l_c is the range $[0, l_c]$ in r over which the magnitude of $S_2^{(2)} - \phi_2^2$ is appreciably fluctuating around zero [19].

A. Equilibrium Hard Spheres

Here we consider the well-known equilibrium distribution of hard spheres of radius a (phase 2) in a matrix (phase 1) [34]. For this model, depicted in Fig. 1(A), all non-overlapping configurations are equally probable. This equilibrium model is athermal, i.e.,

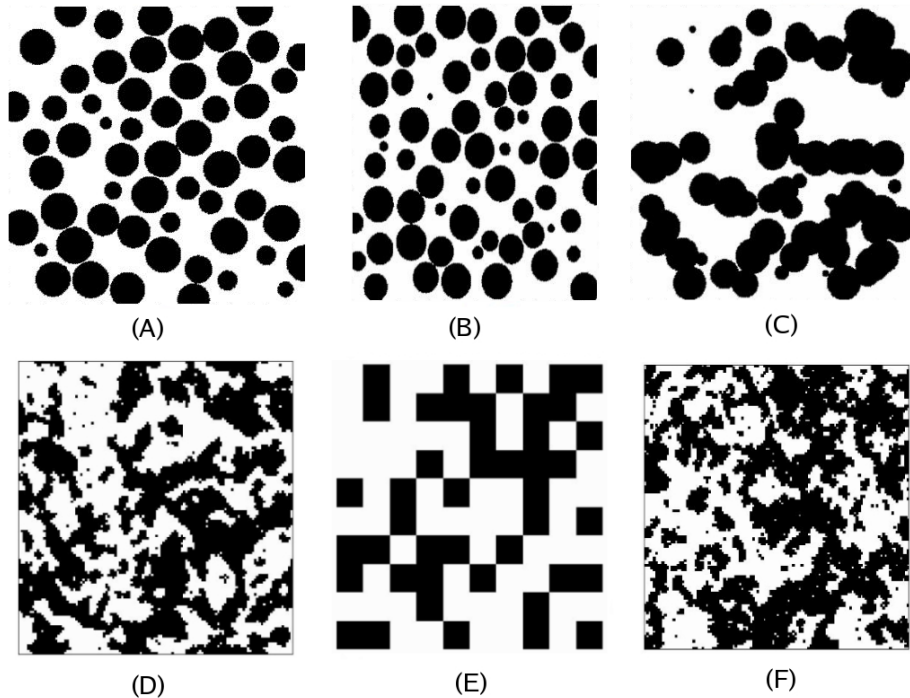


FIG. 1: (Color online) Two-dimensional slices of the three-dimensional microstructures described in this section at volume fraction $\phi_2 = 0.5$. They are hard spheres (A), hard oriented spheroids (B), fully penetrable spheres (C), Debye random media [32] (D), random checkerboard (E) (in any plane perpendicular to a principal axis), and power-law-correlated materials [32] (F). Both the fully-penetrable-sphere model and random checkerboard at $\phi_2 = 0.5$ are above their respective percolation thresholds for the black phase 2, even though planar cuts through these samples do not reveal that the black phase is indeed percolating in three dimensions. We expect that the Debye random medium and power-law-correlated materials shown here also percolate at $\phi_2 = 0.5$.

the behavior of the system is temperature-independent. The pair correlation function $g_2(r)$ for particle centers may be expressed in closed form in Fourier space using the Percus-Yevick approximation, as described in Ref. 19. The two-point function $S_2^{(2)}(r)$ can be obtained from the pair correlation function via the following equation [35]:

$$S_2^{(2)}(r) = \rho v_2^{(int)}(r; a) + \rho^2 g_2 \otimes m \otimes m, \quad (34)$$

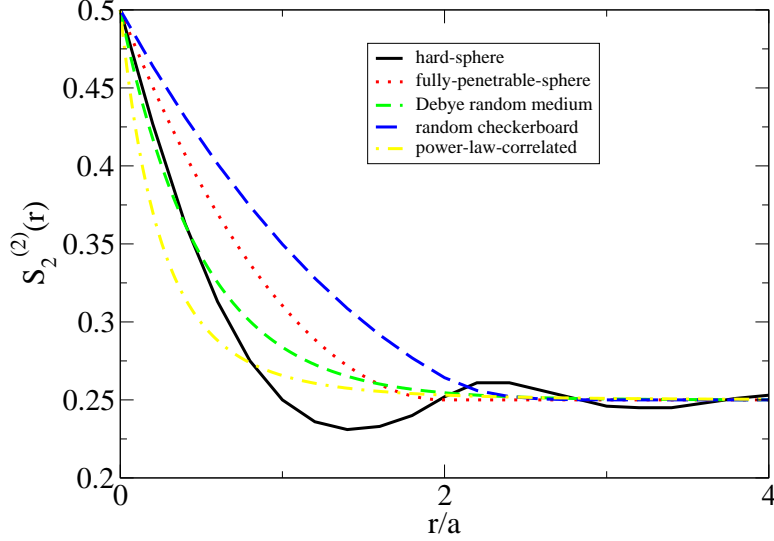


FIG. 2: (Color online) Plots of the two-point correlation function $S_2^{(p)}(r)$ for the five isotropic models detailed in this section: hard spheres, fully penetrable spheres, Debye random medium, random checkerboard, and a power-law-correlated material. The volume fraction for each model is $\phi_2 = 0.5$. Note that the correlation lengths for each model are roughly equal to one another.

where ρ is the number density of spheres, $v_2^{(int)}(r; a)$ is the intersection volume between two spheres of radius a that are a distance r apart, which is given by

$$v_2^{(int)}(r; a) = \begin{cases} 1 - \frac{3}{4}\frac{r}{a} + \frac{1}{16}\left(\frac{r}{a}\right)^3, & \text{if } r < 2a \\ 0, & \text{otherwise} \end{cases}, \quad (35)$$

the symbol \otimes denotes the convolution of two functions, and the step function m is defined by

$$m(\mathbf{r}) = \begin{cases} 1, & \text{if } |\mathbf{r}| < a \\ 0, & \text{otherwise} \end{cases}. \quad (36)$$

Note that the volume fraction of spheres is given by $\phi_2 = \rho 4\pi a^3/3$. The two-point correlation function $S_2^{(2)}(r)$ is plotted in Fig. 2. The most convenient method of obtaining $S_2^{(2)}(r)$ via Eq. (34) is via Fourier transform techniques. The reason for this is that in Fourier space, the convolution operators become simple products, and the Percus-Yevick pair correlation function may be expressed analytically. In order to obtain $S_2^{(2)}(r)$ in real space, numerical inversion from Fourier representation must be performed.

Of all the isotropic disordered models considered here, the hard-sphere system may be thought to possess the greatest degree of order because its coarseness C_∞ is minimized among

the structures considered. For example, consider volume fraction $\phi_2 = 0.5$, at which spheres are slightly above their freezing volume fraction. The correlation function $S_2^{(2)}(r) - \phi_2^2$ exhibits oscillation above and below zero, suggesting strong short-range correlations and anti-correlation among the spheres in the system. Calculations show that as a result of this property, the imaginary component of the dielectric constant is very small compared with that of other model microstructures considered here.

B. Equilibrium Hard Spheroids

We also consider an equilibrium dispersion of hard spheroids (phase 2), or ellipsoids of revolution, in a matrix (phase 1), which are constrained to have the same orientation (see Fig. 1(B)) along the z axis. Because there is an axis of symmetry, spheroids possess azimuthal symmetry. This statistically homogeneous but anisotropic dispersion is considered here in order to demonstrate the application of our formalism to macroscopically anisotropic media, i.e., materials with an effective dielectric tensor with non-equal diagonal terms in the principal axes frame. The spheroid shape is defined by

$$(x^2 + y^2)/a^2 + z^2/b^2 = 1, \quad (37)$$

where a and b are the semi-axes of the spheroid with b being along the axis of symmetry (i.e., z axis). We define the aspect ratio as b/a so that $b/a > 1$ and $b/a < 1$ corresponds to prolate and oblate spheroids, respectively. In a previous work, Torquato and Lado [36] showed that the correlation function for any dispersion of oriented spheroids (in equilibrium or not) at number density ρ could be transformed directly from the hard-sphere correlation function at the same number density by an affine (linear) transformation of the coordinate system. Taking phase 2 to be the spheroid phase, this transform is defined by

$$S_{2,HS}^{(2)}(\mathbf{r}; b/a) = S_{2,HS}^{(2)}[\sigma_0(r_{12}/\sigma(\theta)); 1], \quad (38)$$

where

$$\sigma(\theta) = \frac{2a}{[1 - (1 - a^2/b^2) \cos^2(\theta)]^{1/2}}, \quad (39)$$

where $\sigma_0 = 2a$, θ is the polar angle between the z axis and the radial vector \mathbf{r} , and $S_{2,HS}^{(2)}(\mathbf{r}; 1)$ is the hard-sphere correlation function at the same number density. Here we employ the equilibrium hard-sphere model to get the corresponding expression for the equilibrium hard-oriented-spheroid system.

C. Fully Penetrable Spheres

A fully-penetrable-sphere model is composed of spheres of radius a (phase 2) whose centers are completely uncorrelated in space [19] (see Fig. 1(C)). For this dispersion, the particle phase percolates at $\phi_2 = 0.2895 \pm 0.0005$ [37] (i.e., the medium contains infinite clusters of phase 2), and the matrix phase (phase 1) percolates until a volume fraction of spheres of 97%. The n -point correlation function for this system, for phase 1, is given in Ref. 19 as

$$S_n^{(1)}(\mathbf{r}^n) = \exp[-\rho v_n(\mathbf{r}^n; a)], \quad (40)$$

where the number density ρ is defined here by $\phi_1 = \exp(-\eta)$, with $\eta = \rho 4\pi a^3/3$, and the function $v_n(\mathbf{r}^n; a)$ gives the union volume of n spheres of radius a with centers defined by the position coordinates $\mathbf{r}^n \equiv \mathbf{r}_1, \mathbf{r}_2, \dots, \mathbf{r}_n$. Thus, we may write, for the particle phase,

$$S_2^{(2)}(r) = 1 - 2\phi_2 + \exp\left[-\eta \frac{v_2(r; a)}{v_1(a)}\right], \quad (41)$$

where we have

$$\frac{v_2(r; a)}{v_1(a)} = 2\Theta(r - 2a) + \left[1 + \frac{3r}{4a} - \frac{1}{16} \left(\frac{r}{a}\right)^3\right] \Theta(2a - r), \quad (42)$$

and $\Theta(x)$ is the unit step function. The correlation function $S_2^{(2)}(r)$ is plotted in Fig. 2. Here, we have used the fact that we can relate the union and intersection volume of two spheres by the equation

$$v_2(r; a) = 2v_1(a) - v_2^{(int)}(r; a). \quad (43)$$

The function $S_3^{(2)}$ may be obtained in similar way. It involves an expression for the intersection volume of three spheres, given originally by Powell in Ref. 38, and discussed in detail in Ref. 19. In the next section, we present estimates of the effective dielectric constant as obtained from two- and three-point approximations for this model. Compared with the hard-sphere model, the fully-penetrable-sphere dispersion is significantly more disordered. This is reflected in the appreciably large difference between the imaginary components of their effective dielectric constants, as will be described.

D. Debye Random Medium

The two-point correlation function for a Debye random medium is given by

$$S_2^{(2)}(r) - \phi_2^2 = \phi_2(1 - \phi_2) \exp(-r/\gamma), \quad (44)$$

with $\gamma > 0$. This correlation function is plotted in Fig. 2. In the following analysis, we take $\gamma = a/2$. This correlation function, first proposed by Debye [31], was imagined to correspond to porous media with cavities of random shapes and sizes (a realization of this medium is depicted in Fig. 1(D)). However, it was not known until recently that such a correlation function was indeed realizable by a two-phase medium. Using a “construction” procedure, Yeong and Torquato [32] demonstrated that the correlation function defined in Eq. (44) is realizable and dubbed such systems Debye random media (see also Refs. 19 and [30] for further discussion of the realizability of Debye random media). Note that if the two component dielectrics and their respective volume fractions are interchanged, the correlation function given in Eq. (44) remains invariant. This property is called *phase-inversion symmetry*. A composite is phase-inversion symmetric if the morphology of phase 1 at volume fraction ϕ_1 is statistically identical to that of phase 2 at the same volume fraction, ϕ_1 [19, 32]. None of the sphere and spheroid dispersions possess this property. It is also important to note that the percolation behavior of Debye random media has not been investigated to date. However, based on our knowledge of the percolation threshold of the fully-penetrable-sphere model and visual inspection of the planar cut through a three-dimensional Debye random medium shown in Fig. 1, we expect that the percolation threshold of the latter is substantially below $\phi_2 = 0.5$.

E. Random Checkerboard

The random checkerboard model is produced by partitioning space into cubes such that each cube is assigned phase 1 or phase 2 randomly according to the volume fraction (see Fig. 1(E)). The cubes have side length $D = 2a$. The calculation of the radially averaged two-point correlation function for this model is not presented here. A detailed derivation of this result may be found in Ref. 19. The radially averaged two-point function, $S_2^{(2)}(r)$, is plotted in Fig. 2. This model may be thought of as being more “ordered” than, for example, the Debye random medium because the phases are confined to lie on a grid. In our calculations, presented in the next section, we find that the random checkerboard has a greater imaginary component, however, than that of hard spheres at volume fraction $\phi_2 = 0.5$. This makes intuitive sense: in this regime, the hard-sphere system is near crystallization; there is no such order-disorder transition for the random checkerboard model. As in the Debye random

medium, this model possesses phase-inversion symmetry. For site percolation on a simple cubic lattice with nearest-neighbor connectivity criteria, phase 2 would percolate at a volume fraction of $\phi_2 = 0.312$. However, for the related dielectric and conductivity problems, it is known that edges and corner points will contribute to the effective properties and therefore nearest, next-nearest, and next-next-nearest connectivity criteria must be used. This will result in a substantially lower percolation threshold than $\phi_2 = 0.312$, as one can ascertain from the analogous two-dimensional percolation problem on a square lattice. In summary, the percolation threshold for the three-dimensional random checkerboard should be considerably lower than that for fully penetrable spheres ($\phi_2 = 0.2895$).

F. Power-Law-Correlated Materials

The two-point correlation function for these composites are given by

$$S_2^{(2)}(r) - \phi_2^2 = \frac{\phi_2(1 - \phi_2)a^n}{(r + a)^n}, \quad (45)$$

where the exponent n must obey the inequality $n \geq 3$ for the Fourier transform of the left side of (45) to exist. The two-point correlation function $S_2^{(2)}$ is plotted in Fig. (2) with $n = 4$, which is the value of the exponent that will be considered throughout the rest of the paper. A single realization of a power-law-correlated material with this correlation function is depicted in Fig. 1(F). The degree of correlation in this model is of course highly dependent upon the exponent n . Note that as in the cases of the Debye random medium and the random checkerboard, the power-law-correlated material is phase-inversion symmetric. This correlation function is being put forward in this study for the first time. However, it is not necessarily true that any proposed functional form of S_2 is physically realizable. Any correlation function that corresponds to a realizable material must satisfy a number of necessary conditions [30]. Namely, (1) $0 \leq S_2^{(2)}(\mathbf{r}) \leq \phi_2$, (2) the radial derivative of $S_2^{(2)}$ must be strictly negative at the origin, (3) it must obey the triangle inequality $S_2^{(2)}(\mathbf{r}) \geq S_2^{(2)}(\mathbf{s}) + S_2^{(2)}(\mathbf{t}) - \phi_2$, where $\mathbf{r} = \mathbf{t} - \mathbf{s}$, and (4) the Fourier transform of $S_2^{(2)}(\mathbf{r}) - \phi_2^2$ must be everywhere non-negative. We have tested each of these conditions for the power-law correlation function, and they are all satisfied. For all other models considered in this work have either been known to be realizable or have been recently shown to be [19, 32]. We choose to study power-law-correlated materials because they are reminiscent of structures that are

scale-free. While the correlation function given in Eq. (45) is, strictly speaking, not scale-free (i.e., a function directly proportional to $1/r^n$), it does asymptotically approach this behavior for $r \gg a$. A purely scale-free function does not satisfy the known realizability constraints. Model microstructures that have scale-free correlation functions exhibit interesting clustering and percolation properties [19]. This model’s percolation behavior will be studied in greater detail in a forthcoming study [33]. As in the case of the Debye random medium, percolation behavior of power-law-correlated materials has not been investigated to date. However, for the same reasons given in Section III.D, we expect that the percolation threshold of the latter is substantially below $\phi_2 = 0.5$.

IV. RESULTS

In this section, we present results for the effective dielectric constant as predicted by the two-point approximation (32) for each of the model microstructures discussed in the previous section, i.e., hard spheres, hard oriented spheroids, fully penetrable spheres, Debye random media, random checkerboard, and power-law-correlated materials (with exponent $n = 4$). Henceforth, we take $\varepsilon_2 \geq \varepsilon_1$, and assume both ε_1 and ε_2 are real. We take the wave number for a wave propagating through phase 1 to be $2\pi/(60a)$. If phase 1 has dielectric constant 1, then this corresponds to a propagation frequency of 5 GHz. For reasons given in Section II.C, we take $q = 1$ and $p = 2$ if phase 2 is below its percolation threshold, and we take $p = 1$ and $q = 2$ if it is above its percolation threshold. In the case of the fully-penetrable-sphere model, we also evaluate the three-point approximation (33).

A. Two-Point Estimates

1. Isotropic Media

For the hard-sphere model, we employ the two-point approximation given in Eq. (32) with $q = 1$ and $p = 2$ where the spheres comprise phase 2, for $\phi_2 \leq 0.5$ (see discussion in Section II.C). This choice of two-point approximation is expected to be accurate because the equilibrium hard-sphere model percolates at “jammed” states, which are substantially higher than $\phi_2 = 0.5$ [19]. In the case of the fully-penetrable-sphere model, we plot our results for a fixed phase contrast ratio but over the entire volume fraction range because in

this case we know its nontrivial percolation threshold (see Section III.C). For this model, we expect (32) with $p = 2$ and $q = 1$ to be valid for volume fractions well below its percolation threshold of $\phi_2 = 0.2895$, and then with $p = 1$ and $q = 2$ to be valid well above it. In the intermediate region, which is taken to be $0.2 < \phi_2 < 0.4$, we interpolate between these two regimes using a spline fit in order to approximately account for the fact that this medium is crossing its percolation threshold. For Debye random media, random checkerboard, and power-law-correlated materials (in which we take the exponent $n = 4$), the percolation thresholds are not known. Therefore, we limit ourselves to analyzing the effective dielectric constant of these models for volume fractions that are assumed to be below these thresholds (e.g., $\phi_2 = 0.1$), and well above them (e.g., $\phi_2 = 0.5$). In the former case, we use the two-point approximation (32) with $p = 2$ and $q = 1$, and in the latter case with $p = 1$ and $q = 2$. For all of the five isotropic models, we employ the two-point estimate (32) with the expansion given in Eq. (29) through third order in k_q , and choose the correlation lengths to be roughly equal to one another. Different two-point approximations are employed for the various statistically homogeneous and isotropic model microstructures below and above their percolation thresholds for reasons given at the end of Section II.C.

For the disordered models described in Section III, we present in Table I the two lowest-order coefficients of $k_q a$ in the expansion of $A_2^{(p)}$, as given in Eq. (29). Note that the zeroth-order term is zero, because $A_2^{(p)}$ is zero in the isotropic static problem. As can be seen from Eq. (28), there can be no first-order term either. The second-order term is necessarily real, and the third-order term necessarily imaginary. We call the j^{th} order coefficient in this expansion $\alpha_j^{(2)}$, such that $A_2^{(p)} = \sum_{j=2}^{\infty} \alpha_j^{(2)} (k_q a)^j$.

In Figs. 3 and 4, we show the real and imaginary components of the effective dielectric constant, respectively, of five isotropic models described in the previous section, plotted against dielectric-contrast ratio at a volume fraction $\phi_2 = 0.1$. Since each model is below or assumed to be below its percolation threshold at this volume fraction, the two-point approximation (32) is used in conjunction with (29) in order to calculate $A_2^{(p)}$. The real and imaginary parts of the effective dielectric constant at volume fraction $\phi_2 = 0.5$ are plotted in Figs. 5 and 6, respectively. At this volume fraction, all structures except for the hard-sphere model are above their percolation thresholds. As shown in Fig. 4, the imaginary component of the effective dielectric constant of the hard-sphere model is significantly smaller than that of the fully-penetrable-sphere model. This makes intuitive sense because the constraint

	HS		FPS		DRM		RC		PLC	
	$\alpha_2^{(2)}$	$\alpha_3^{(2)}$	$\alpha_2^{(2)}$	$\alpha_3^{(2)}$	$\alpha_2^{(2)}$	$\alpha_3^{(2)}$	$\alpha_2^{(2)}$	$\alpha_3^{(2)}$	$\alpha_2^{(2)}$	$\alpha_3^{(2)}$
$\phi_2 = 0.1$	0.0512	0.0304 <i>i</i>	0.0700	0.0579 <i>i</i>	0.0450	0.0450 <i>i</i>	0.108	0.116 <i>i</i>	0.0300	0.0600 <i>i</i>
$\phi_2 = 0.2$	0.0658	0.0279 <i>i</i>	0.120	0.0990 <i>i</i>	0.0800	0.0800 <i>i</i>	0.193	0.206 <i>i</i>	0.0533	0.1067 <i>i</i>
$\phi_2 = 0.3$	0.0625	0.0188 <i>i</i>	0.152	0.124 <i>i</i>	0.1050	0.1050 <i>i</i>	0.253	0.270 <i>i</i>	0.0700	0.1400 <i>i</i>
$\phi_2 = 0.4$	0.0512	0.0107 <i>i</i>	0.165	0.134 <i>i</i>	0.1200	0.1200 <i>i</i>	0.289	0.308 <i>i</i>	0.0800	0.1600 <i>i</i>
$\phi_2 = 0.5$	0.0383	0.0052 <i>i</i>	0.163	0.130 <i>i</i>	0.1250	0.1250 <i>i</i>	0.301	0.321 <i>i</i>	0.0833	0.1667 <i>i</i>
$\phi_2 = 0.6$			0.146	0.115 <i>i</i>	0.1200	0.1200 <i>i</i>	0.289	0.308 <i>i</i>	0.0800	0.1600 <i>i</i>
$\phi_2 = 0.7$			0.116	0.0894 <i>i</i>	0.1050	0.1050 <i>i</i>	0.253	0.270 <i>i</i>	0.0700	0.1400 <i>i</i>
$\phi_2 = 0.8$			0.0770	0.0575 <i>i</i>	0.0800	0.0800 <i>i</i>	0.193	0.206 <i>i</i>	0.0533	0.1067 <i>i</i>
$\phi_2 = 0.9$			0.0339	0.0239 <i>i</i>	0.0450	0.0450 <i>i</i>	0.108	0.116 <i>i</i>	0.0300	0.0600 <i>i</i>

TABLE I: Coefficients of the $(k_q a)^2$ and $(k_q a)^3$ terms in the expansion of $A_2^{(p)}$ (given in Eq. (29)), for each of the isotropic models considered here. These are the hard-sphere (HS) model, fully-penetrable-sphere (FPS) system, Debye random medium (DRM), random checkerboard (RC), and a power-law-correlated system (PLC). For hard spheres and fully penetrable spheres, the spheres comprise phase 2. The parameter $\alpha_j^{(2)}$ is the j^{th} -order coefficient. As demonstrated in Eq. (28), there are no zeroth or first order terms in this expansion.

that hard spheres may not overlap results in larger spatial correlations (smaller coarseness), leading to a smaller imaginary component. Upon increasing volume fraction, the hard-sphere model becomes less and less coarse. Close to its freezing point, at $\phi_2 \approx 0.5$, the resulting imaginary component of ε_e is extremely small, as shown in Fig. 6. At volume fraction $\phi_2 = 0.5$, the real part of ε_e for the hard sphere model is significantly smaller than that of the other models, since it is the only one that is not percolating. As Fig. 6 shows, the imaginary component of the effective dielectric constant is substantially more sensitive to microstructure than the corresponding real component of ε_e .

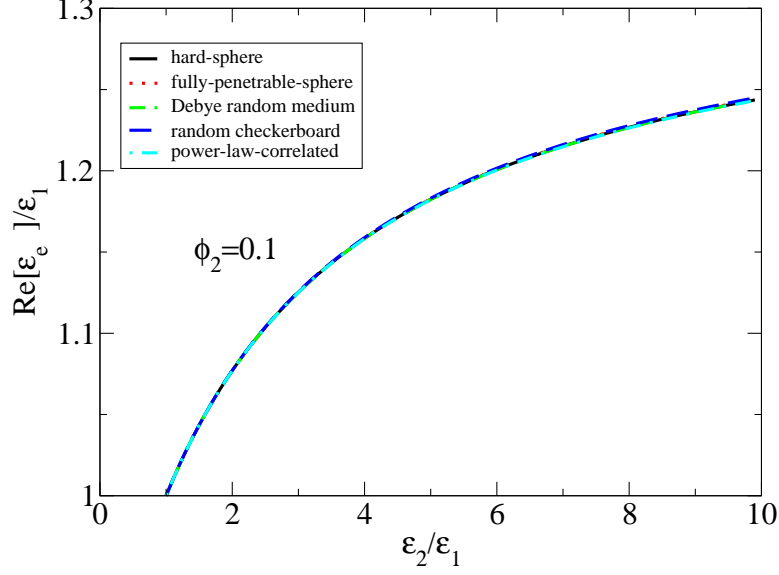


FIG. 3: (Color online) Real part of the effective dielectric constant of the various isotropic models studied here as a function of dielectric-contrast ratio $\varepsilon_2/\varepsilon_1$ at volume fraction $\phi_2 = 0.1$ and wave number $k_1 = 2\pi/(60a)$. For all models, the two-point approximation (32) with $p = 2$ and $q = 1$ is used since they are each below or assumed to be below their percolation thresholds. In order to calculate $A_2^{(p)}$ for each microstructure, Eq. (29) is used.

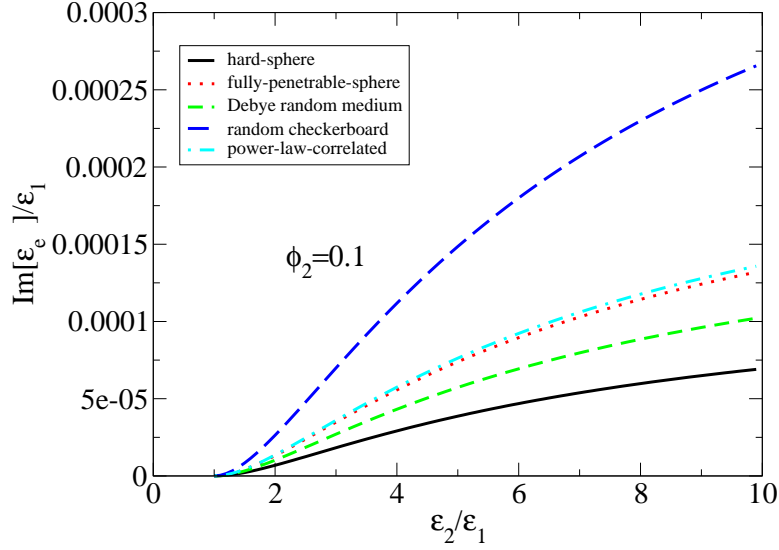


FIG. 4: (Color online) Corresponding imaginary part of the effective dielectric constant for the isotropic models depicted in Fig. 3.

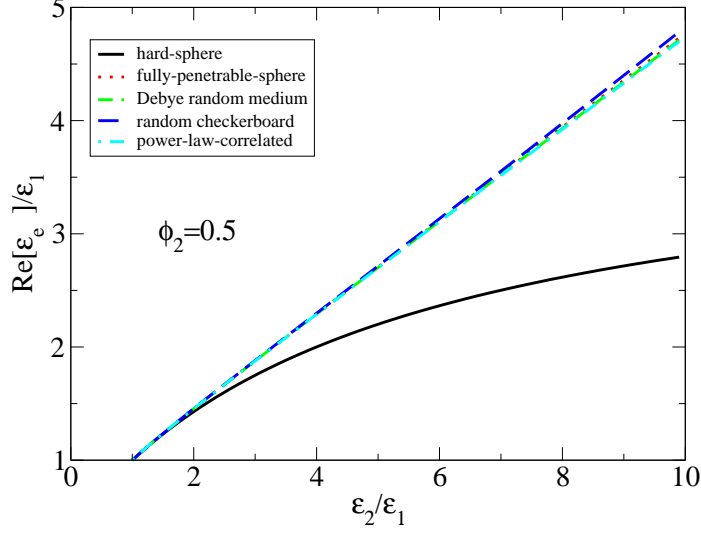


FIG. 5: (Color online) Real part of the effective dielectric constant of the various isotropic models studied here as a function of dielectric-contrast ratio $\varepsilon_2/\varepsilon_1$ at volume fraction $\phi_2 = 0.5$ and wave number $k_1 = 2\pi/(60a)$. For all of the models besides hard spheres, the two-point approximation (32) with $p = 1$ and $q = 2$ is used, since they are each above their percolation thresholds. For the hard-sphere model, which is below its percolation threshold, we use (32) with $p = 2$ and $q = 1$. Eq. (29) is used to calculate $A_2^{(p)}$,

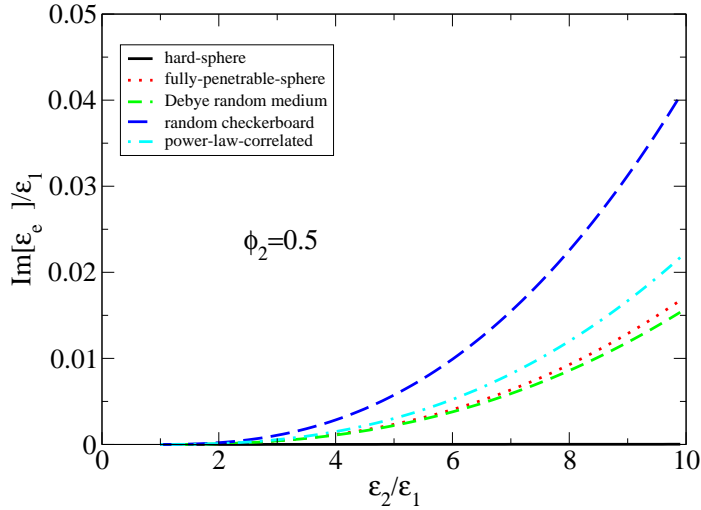


FIG. 6: (Color online) Corresponding imaginary part of the effective dielectric constant of the isotropic models depicted in Fig. 5. On the scale of this figures, the hard-sphere curve is almost indistinguishable from the horizontal axis.

In Figs. 7 and 8, we plot the real and imaginary components of ε_e for the fully-penetrable-sphere model as a function of volume fraction. The two-point approximation (32) is used, with $p = 2$ and $q = 1$ for $0 \leq \phi_2 \leq 0.2$ (which is below the percolation threshold of $\phi_2 = 0.2895$), and $p = 1$ and $q = 2$ for $0.4 \leq \phi_2 \leq 1$. A spline fit is used to interpolate between these two curves to yield an approximation for $0.2 < \phi_2 < 0.4$. Eq. (29) is used to calculate $A_2^{(p)}$.

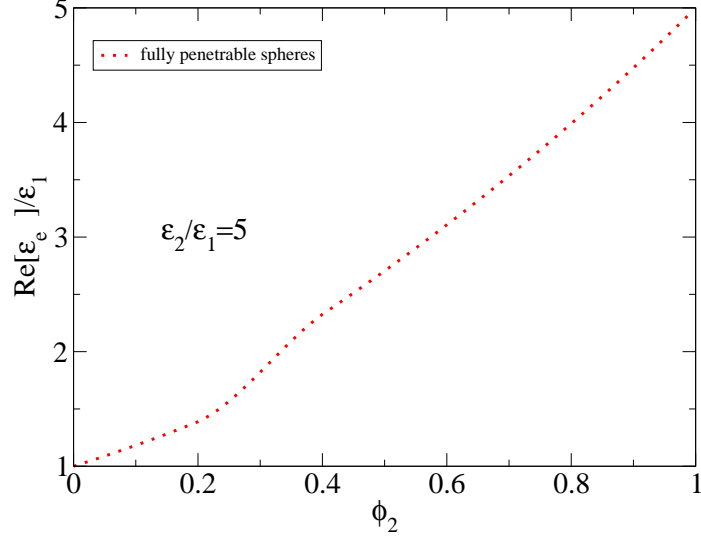


FIG. 7: (Color online) Real part of the effective dielectric constant of the fully-penetrable-sphere model as a function of volume fraction ϕ_2 of phase 2 at a dielectric contrast ratio $\varepsilon_2/\varepsilon_1 = 5$ and at wave number $k_1 = 2\pi/(60a)$. The two-point approximation (32) is used with $p = 2$ and $q = 1$ below the percolation threshold of $\phi_2 = 0.2895$, and $p = 1$ and $q = 2$ above it. A spline fit is used to interpolate between these two formulas and Eq. (29) is used to calculate $A_2^{(p)}$.

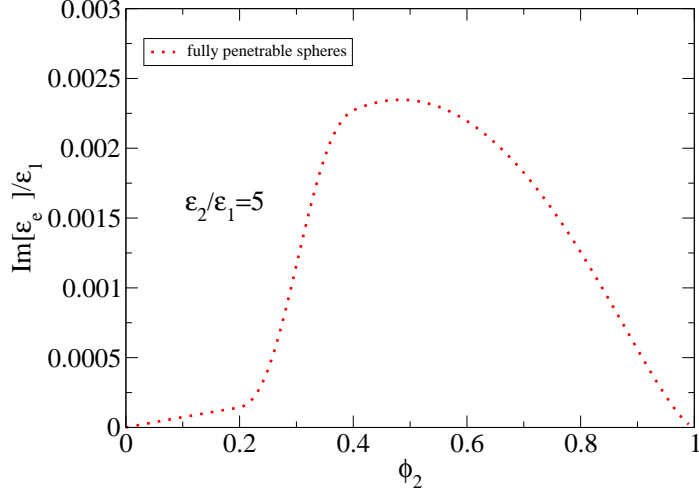


FIG. 8: (Color online) Corresponding imaginary part of the effective dielectric constant for the fully-penetrable-sphere model depicted in Fig. 7. A spline fit is used to interpolate between the two formulas.

Among the isotropic model microstructures that are discussed here, it is possible to carry out the full $A_2^{(p)}$ integral as given in Eq. (28), rather than the expansion given in Eq. (29). That said, since for both the real and the imaginary parts of $A_2^{(p)}$, the next term in the expansion is smaller by a factor of $(k_q a)^2$, Eq. (29) gives an extremely good approximation to the effective dielectric constant at long wavelength.

2. Anisotropic Media

Drawing upon results discussed in Appendix C in which we apply our formalism at the two-point level to calculate the effective dielectric tensor of statistically anisotropic with azimuthal symmetry, we present results for the axial and planar dielectric constants for an equilibrium dispersion of hard oriented spheroids in a matrix for a number of spheroid aspect ratios, as predicted by the two-point approximation, given in Eqs. (C1) and (C6). Figures 9 and 10 show real and imaginary component results, respectively, for the anisotropic hard-spheroid model, giving axial and in-plane dielectric constants of the composite in each plot, as predicted by the two-point approximation, given in Eqs. (C1) and (C6). The former plot, Fig. 9 shows that upon increasing the aspect ratio b/a , the axial component of the dielectric tensor increases. This makes intuitive sense because in the purely static case,

as the microstructure approaches the long-needle limit, the tensor component in the axial direction should approach the arithmetic mean $(\sigma_1\phi_1 + \sigma_2\phi_2)$, which is a rigorous upper bound on the effective dielectric constant in the purely static case. We see that the in-plane component decreases with increasing aspect ratio. We may again understand this in the context of the static regime: in that scenario, the two-point tensor $\mathbf{A}_2^{(p)}$ must remain traceless. The decreasing in-plane component is a direct result of this property and the fact that the axial component increases with aspect ratio. By contrast, we see from Fig. 10 that both the axial and in-plane imaginary parts of the dielectric tensor increase with increasing aspect ratio.

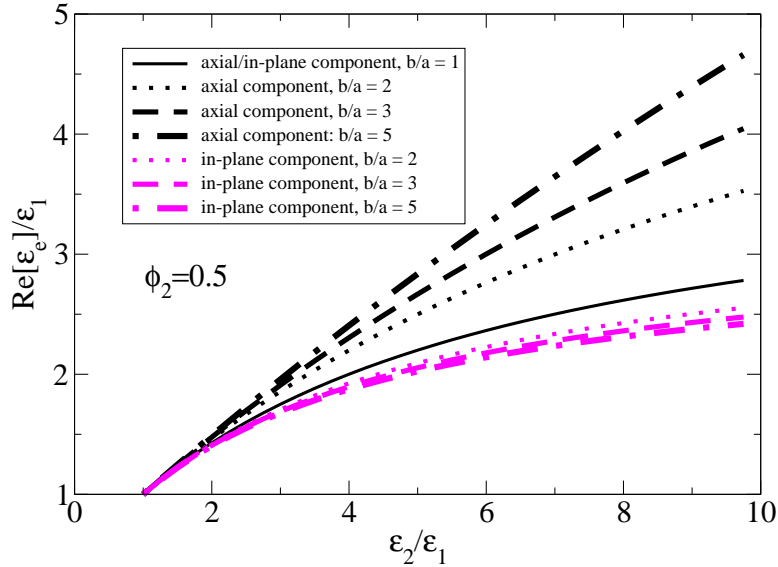


FIG. 9: (Color online) Real part of the axial and transverse effective dielectric constants of an equilibrium dispersion of hard oriented prolate spheroids, plotted as a function of dielectric-contrast ratio ϵ_2/ϵ_1 , for a number of different aspect ratios b/a , as predicted by the two-point approximation, given in Eqs. (C1) and (C6). The contrast is $\epsilon_2/\epsilon_1 = 5$, the volume fraction is $\phi_2 = 0.5$, and $k_1 = 2\pi/(60a)$, where a is the semi-minor axis of the spheroid.

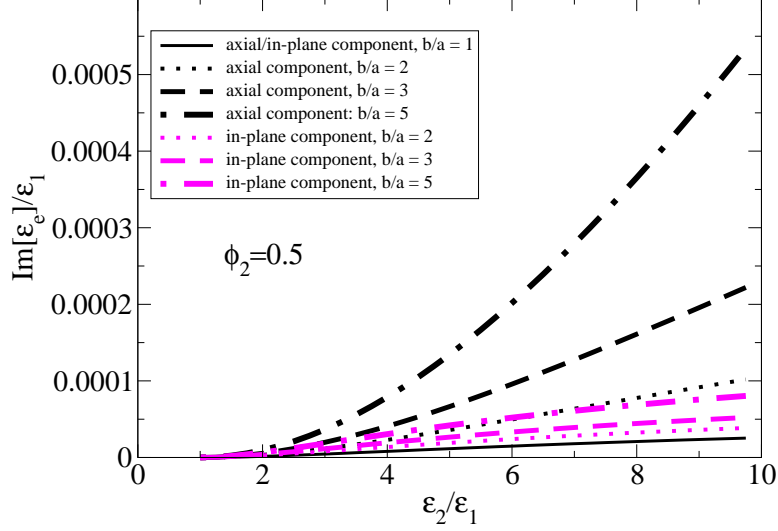


FIG. 10: (Color online) The corresponding imaginary part of the axial and transverse effective dielectric constants for the same model and cases depicted in Fig. 9.

Although we do not show results for the oblate case, we have verified that as the aspect ratio of the spheroids is increased from the oblate regime ($b/a < 1$) through the prolate regime ($b/a > 1$), the real part of the axial dielectric constant increases and the real part of the in-plane dielectric constant decreases, which agrees the behavior given in Ref. 36. The imaginary components of both the axial and in-plane dielectric constants both increase with increasing aspect ratio.

B. Three-Point Estimates

Here we apply the isotropic three-point approximation, given explicitly in Eq. (33), (with $p = 1$ and $q = 2$) to the fully-penetrable-sphere model in order to ascertain the importance of three-point information. For this model, Table II gives the coefficients of $(k_q a)$ for the first two terms of $A_3^{(p)}$, as given in Eq. (31), for a number of volume fractions. We call the j^{th} order coefficient in this expansion $\alpha_j^{(3)}$, such that $A_3^{(p)} = \sum_{j=0}^{\infty} \alpha_j^{(3)} (k_q a)^j$.

The importance of three-point information at high contrast and volume fraction is demonstrated in Figs. 11 and 12, which give the $(k_1 a)^2$ and $(k_1 a)^3$ coefficients of the effective dielectric constant of the fully-penetrable-sphere model at $\phi_2 = 0.5$, which is well above its percolation threshold. The effective dielectric constant is calculated via the two-point

	$p = 2, q = 1$		$p = 1, q = 2$	
	$\alpha_0^{(3)}$	$\alpha_2^{(3)}$	$\alpha_0^{(3)}$	$\alpha_2^{(3)}$
$\phi_p = 0.1$	0.010	0.012	0.079	0.013
$\phi_p = 0.2$	0.035	0.040	0.17	0.043
$\phi_p = 0.3$	0.070	0.075	0.24	0.085
$\phi_p = 0.4$	0.11	0.11	0.31	0.13
$\phi_p = 0.5$	0.14	0.13	0.35	0.17
$\phi_p = 0.6$	0.17	0.15	0.37	0.20
$\phi_p = 0.7$	0.17	0.14	0.35	0.21
$\phi_p = 0.8$	0.15	0.11	0.28	0.18
$\phi_p = 0.9$	0.10	0.053	0.17	0.12

TABLE II: Coefficients of the $(k_q a)^0$ and $(k_q a)^2$ terms in the expansion of $A_3^{(p)}$ (given in Eq. (31)), for the fully-penetrable-sphere model, where the spheres comprise phase 2. The parameter $\alpha_j^{(3)}$ is the j^{th} -order coefficient. As demonstrated in Eq. (31), there are no first- or third- order terms in this expansion.

and three-point approximations, given in Eqs. (32) and (33), respectively. These equations employ the expansions given in Eqs. (29) and (31). For this model, we have taken $q = 2$ and $p = 1$. Clearly, for both the $(k_1 a)^2$ coefficient (which is real), and the $(k_1 a)^3$ (which is imaginary), three body information plays a significant role at high volume fraction and contrast. We also plot the imaginary component of the effective dielectric constant for this model, both with and without the third-order contribution in Fig. 13. We see that up to a dielectric-contrast ratio of roughly 5, the two-point and three-point approximations are in relatively good agreement, but afterwards they increasingly diverge. This serves as a test of the convergence of the series. We thus see that up to relatively high contrast ratio (i.e., $\varepsilon_2/\varepsilon_1 \approx 5$), the two-point approximation provides a good estimate, implying that the remaining terms in the full series expansion (19) are negligibly small.

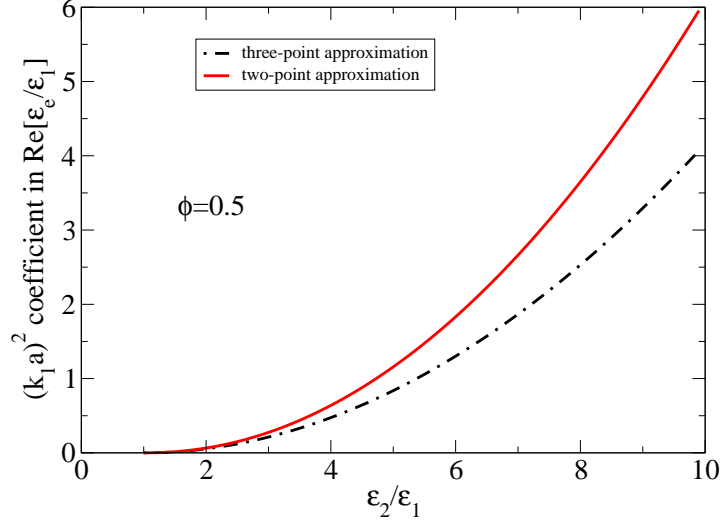


FIG. 11: (Color online) The coefficient of $(k_1 a)^2$ of the effective dielectric constant as a function of dielectric-contrast ratio in the fully-penetrable-sphere model at volume fraction $\phi_2 = 0.5$, as predicted by the two-point and three-point approximations, given in Eqs. (32) and (33), respectively. We take $p = 1$ and $q = 2$ since the system is above its percolation threshold at this volume fraction. These equations employ the expansions given in Eqs. (29) and (31). This term is necessarily real. The solid and dashed curves show this quantity with and without the three-point term included in the expansion given in Eq. (17).

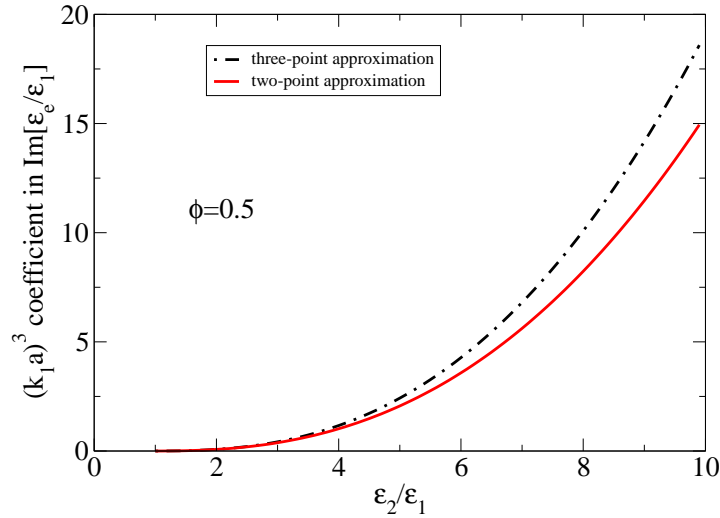


FIG. 12: (Color online) As in Fig. 11, except for the coefficient of $(k_1 a)^3$.

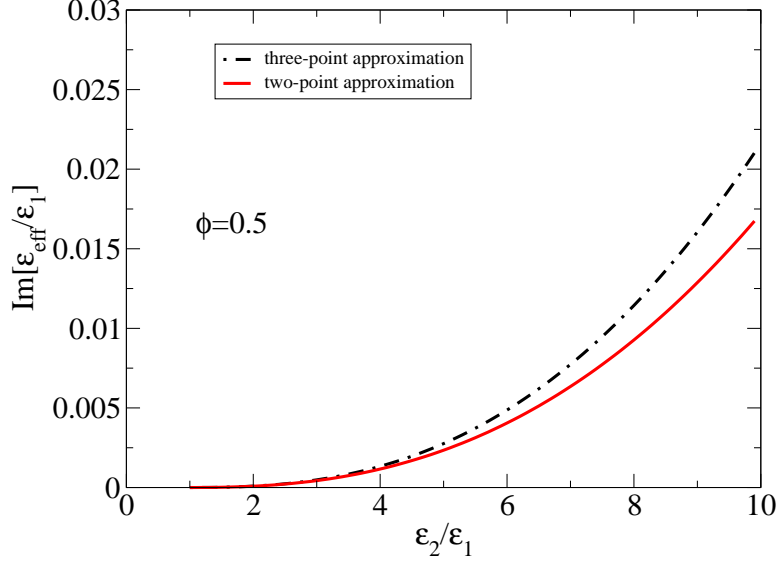


FIG. 13: (Color online) The imaginary part of the effective dielectric constant of the fully-penetrable-sphere model at volume fraction $\phi_2 = 0.5$ and wave number $k_1 = 2\pi/(60a)$, as predicted by the two-point and three-point approximations, given in Eqs. (32) and (33), respectively. We take $p = 1$ and $q = 2$ since the system is above its percolation threshold at this volume fraction. These equations employ the expansions given in Eqs. (29) and (31). The solid and dashed curves show this quantity with and without the three-point term included in the expansion given in Eq. (17).

V. CONCLUSIONS

We have derived exact strong-contrast expansions (19) for the effective dielectric tensor ϵ_e of electromagnetic waves propagating in a two-phase composite random medium with complex-valued isotropic components in the long-wavelength regime. These expansions are not formal but rather are explicitly given in terms of certain integrals over the n -point correlation functions that statistically characterize the medium. To our knowledge, such an exact representation has not been given explicitly before. The nature of the strong-contrast expansion parameter results in a radius of convergence of the series (19) that is significantly widened beyond that of a weak-contrast expansion (i.e., the simple difference of the dielectric constants of the two phases). Because the expansions can be considered to be perturbations about the solutions of the dielectric tensor of certain optimal structures, we argued that

the first few terms of the expansion (19) should yield a reasonable approximation of ϵ_e , depending on whether the high-dielectric phase is below or above its percolation threshold. In particular, truncations of the exact expansion led to two- and three-point approximations for ϵ_e , which we applied to a variety of different three-dimensional model microstructures, including dispersions of hard spheres, hard oriented spheroids and fully penetrable spheres as well as Debye random media, random checkerboard, and power-law-correlated materials.

We paid special attention in our analysis to case in which the components have real dielectric constants but where the effective dielectric tensor possesses imaginary components due to disorder, a phenomenon which is essential to applications such as remote sensing (e.g. in the calculation of the backscattering coefficient [11]). In examining two-point approximations of the effective dielectric constant for statistically homogeneous and isotropic media with component phases having purely real dielectric constants, we found that the imaginary part of ϵ_e is related to the coarseness for very large windows, which may be regarded to be a crude measure of disorder. Among other results, we found that the equilibrium hard-sphere model for volume fractions up to its freezing point exhibit a much smaller imaginary component of the effective dielectric constant than the other four statistically homogeneous and isotropic model microstructures studied here.

For dispersions of fully penetrable spheres, we analyzed the behavior of the effective dielectric constant using the two- and three-point approximations, Eqs. (32) and (33), respectively. Our results suggest that truncation of the exact expansion (19) at the two-point level yields good convergence up to relatively high phase-contrast ratios (≈ 5). However, the two approximations increasingly diverge from one another for higher values, showing the importance of using three-point information at sufficiently high contrast ratios.

In order to demonstrate the application of our formalism to a statistically anisotropic and hence macroscopically anisotropic media, we examined dispersions of equilibrium hard spheroids. It was shown that as the aspect ratio b/a was increased, the real parts of the axial dielectric constant and the in-plane dielectric constants increased and decreased, respectively. The imaginary components of the axial and in-plane dielectric constants were both found to increase upon increasing the aspect ratio b/a from 1 (i.e., sphere point).

The dichotomy between periodic media, which have zero imaginary component in their effective dielectric constants, and disordered media, which do have such a component, begs an important question: which is true of quasiperiodic structures? These structures possess long-

range order but have no translational symmetry, are therefore in a sense intermediate between the latter two regimes. In Appendix B, we show that at the two-point level, an imaginary component is obtained only if the Fourier transform of the correlation function is nonzero at k_q . For two-phase media with periodic structure (i.e., crystals), this implies that at this level there is no imaginary component, but this argument does not hold for media with quasiperiodic structure (i.e., quasicrystals) [40]. Since the diffraction pattern for quasicrystals possess only discrete Bragg peaks, the coarseness is necessarily zero. However, this does not imply that the imaginary component of ϵ_e is identically zero, since higher-order k_q coefficients may contribute. The calculation of the effective properties of quasicrystal two-phase media and a fundamental understanding of their wave propagation properties remains a challenging open question.

In future work, we plan on applying the strong-contrast formalism of this paper to a number of new model microstructures and explore other comparison materials in the spirit of Ref. 27 to yield even better approximations for ϵ_e . The procedure presented here is applicable in any dimension and is thus well suited to the study of scalar Helmholtz equation for arbitrary space dimension. One application of this case lies in the calculation of effective properties of phononic systems. Another possible extension involves generalizing analogous elastostatic results [19, 39] to the dynamic case.

Acknowledgments

The authors are grateful for useful discussions with Paul Chaikin and Ping Sheng. This work was supported by the Air Force Office of Scientific Research under Grant No. F49620-03-1-0406 and the National Science Foundation under Grant No. DMR-0606415. M. R. acknowledges the support of the Natural Sciences and Engineering Research Council of Canada.

APPENDIX A: TWO-POINT EXPANSION FOR ARBITRARY COMPARISON MATERIAL

The strong-contrast expansion (19) for the effective dielectric tensor was derived for the choice of the comparison material such that $\epsilon_0 = \epsilon_q$ ($q = 1$ or 2). This choice sig-

nificantly simplifies the analysis and has the desirable feature that it can be regarded to be a solution that perturbs around the effective dielectric tensor for certain optimal microstructures. However, for other microstructures, different comparison materials may offer advantages in terms of better series convergence [19, 26] and more accurate approximations [27]. Here we present an equivalent relation to Eq. (32) for macroscopically isotropic media but for an arbitrary comparison material with dielectric constant ε_0 :

$$\frac{1}{\beta_{e0}} = \frac{1}{\beta_{q0} + (\beta_{p0} - \beta_{q0})\phi_p} - \frac{(\beta_{p0} - \beta_{q0})^2}{(\beta_{q0} + (\beta_{p0} - \beta_{q0})\phi_p)^2} A_2^{(p)}, \quad (\text{A1})$$

where $\beta_{e0} = (\varepsilon_e - \varepsilon_0)/(\varepsilon_e + 2\varepsilon_0)$, $\beta_{p0} = (\varepsilon_p - \varepsilon_0)/(\varepsilon_p + 2\varepsilon_0)$, and $\beta_{q0} = (\varepsilon_q - \varepsilon_0)/(\varepsilon_q + 2\varepsilon_0)$. In Ref. 11, ε_0 is taken to be the Bruggeman effective dielectric constant, but this is not the best choice for general microstructures [10]. For example, for the large class of dispersions discussed in Section II.C, the choice $\varepsilon_0 = \varepsilon_q$ is better.

APPENDIX B: PROOF THAT A_2 IS PURELY REAL AT THE TWO-POINT LEVEL

All of the random media studied here have had dielectric tensors with non-zero imaginary component. Thus, electromagnetic waves propagating through these materials will attenuate, albeit with small decay constants. Roughly speaking, the physical cause for this attenuation is the fact that the waves are scattered off of the heterogeneities, and the scattered waves are no longer coherent with the propagating wave, and thus, this energy is “lost”, when homogenization is applied in Eq. (14). However, this is not so for periodic heterogeneous media. In the language of solid-state physics, scattering does not take place because waves are allowed to propagate coherently as Bloch waves (as opposed to in the form of pure plane waves). In this Appendix, we show this explicitly at the two-point level. Although a single periodic configuration is statistically inhomogeneous, our formulation (valid for statistically homogeneous media) can still be applied by first performing a translational average, i.e., averaging over uniformly random displacements of the origin. This produces averaged quantities, such as the correlation function defined by Eq. (25), translationally invariant. Thus, invoking an ergodic hypothesis [19], the ensemble average is equal to an infinite-volume average over the variable \mathbf{r}_1 of a single (periodic) realization. We limit ourselves here to periodic media that yield macroscopically isotropic dielectric tensors.

The two-point coefficient (28) in the macroscopically isotropic case can be written as follows:

$$A_2^{(p)} = \frac{2k_q^2}{(4\pi)} \int d\mathbf{r} \frac{e^{ik_q r}}{r} \left[S_2^{(p)}(\mathbf{r}) - \phi_p^2 \right]. \quad (\text{B1})$$

We define a “difference indicator function” as follows:

$$V(\mathbf{r}) = \mathcal{I}^{(p)}(\mathbf{r}) - \phi_p \quad (\text{B2})$$

such that $\left(S_2^{(p)}(\mathbf{r}) - \phi_p^2 \right) = \langle V(\mathbf{R})V(\mathbf{R} + \mathbf{r}) \rangle$, where the average is taken over the dummy variable \mathbf{R} .

Representing this real-space correlation function in its spectral form, we have

$$\langle V(\mathbf{R})V(\mathbf{R} + \mathbf{r}) \rangle = \int \frac{d\mathbf{q}}{(2\pi)^3} \tilde{V}(\mathbf{q}) \tilde{V}(-\mathbf{q}) \exp(i\mathbf{q} \cdot \mathbf{r}). \quad (\text{B3})$$

where $\tilde{V}(\mathbf{q})$ is the Fourier transform of the difference indicator function at wave vector \mathbf{q} . Inserting this expression into Eq. (B1), we have

$$\begin{aligned} A_2^{(p)} &= \frac{2k_q^2}{(4\pi)} \int d\mathbf{r} \frac{e^{ik_q r}}{r} \int \frac{d\mathbf{q}}{(2\pi)^3} \tilde{V}(\mathbf{q}) \tilde{V}(-\mathbf{q}) \exp(i\mathbf{q} \cdot \mathbf{r}) \\ &= \frac{2k_q^2}{(4\pi)} \int \frac{d\mathbf{q}}{(2\pi)^3} \tilde{V}(\mathbf{q}) \tilde{V}(-\mathbf{q}) \int d\mathbf{r} \exp(i\mathbf{q} \cdot \mathbf{r}) \frac{e^{ik_q r}}{r}. \end{aligned} \quad (\text{B4})$$

We see that the inner integral is just the Fourier transform of the Green’s function of the Helmholtz equation. This inner integral is thus simply $4\pi/(q^2 - k_q^2)$. Thus, taken together, we have

$$A_2^{(p)} = \frac{2k_q^2}{(4\pi)} \int \frac{d\mathbf{q}}{(2\pi)^3} \tilde{V}(\mathbf{q}) \tilde{V}(-\mathbf{q}) \frac{4\pi}{q^2 - k_q^2} \quad (\text{B5})$$

We can see that there are two poles in the last integral located at $q = \pm k_q$. Clearly, for a periodic medium, $\tilde{V}(\mathbf{q})\tilde{V}(-\mathbf{q})$ is identically zero at every point, save the reciprocal lattice vectors, where there are delta functions. If we assume long wavelength, then $k_q \ll G$, where G is the magnitude of the smallest non-zero reciprocal lattice vector. Thus, the pole will not enter in to the calculation! This proves that there can be no imaginary component to this integral, and this must be the case for all periodic structures. For the case of a random medium, since there are indeed correlations at long wavelength (of which there are of course none in the periodic case), there is a non-zero residue at the pole, and the integral can be complex.

APPENDIX C: $\mathbf{A}_2^{(p)}$ FOR AZIMUTHAL SYMMETRY

We now discuss how to explicitly express the tensor two-point coefficient $\mathbf{A}_2^{(p)}$ [cf. (21)] for statistically anisotropic media with an axis of symmetry (say, the z axis) i.e., azimuthal symmetry. An example of such a microstructure is a dispersion of hard oriented spheroids, which we discussed in Section III.C. Here we follow the methodology of Torquato and Lado [36], who evaluated similar integrals for the purely static case. If we align the Cartesian coordinate system with the principal axes frame, the two-point coefficient $\mathbf{A}_2^{(p)}$ is diagonal, i.e.,

$$\mathbf{A}_2^{(p)} = \begin{pmatrix} U & 0 & 0 \\ 0 & U & 0 \\ 0 & 0 & V \end{pmatrix} \quad (\text{C1})$$

where U is the in-plane (i.e., x - y plane) component and V is the axial (z axis) component. We may explicitly write the two-point tensor as

$$\mathbf{A}_2^{(p)} = \frac{3}{4\pi} \int d\mathbf{r} \exp(ik_q r) \frac{(3 - 3ik_q r - k_q^2 r^2)\hat{\mathbf{r}}\hat{\mathbf{r}} + (-1 + ik_q r + k_q^2 r^2)\mathbf{I}}{r^3} \left[S_2^{(p)}(\mathbf{r}) - \phi_p^2 \right] \quad (\text{C2})$$

where we have inserted the dyadic Green's function explicitly. Retaining terms through order k_q^3 , gives the following explicit expressions for U and V in spherical coordinates:

$$\begin{aligned} U = & \frac{3}{4\pi} \int \frac{d\mathbf{r}}{r^3} \left(-1 + \frac{3}{2} \sin^2(\theta) \right) \left[S_2^{(p)}(\mathbf{r}) - \phi_p^2 \right] + \frac{k_q^2}{2} \frac{3}{4\pi} \int \frac{d\mathbf{r}}{r} \left(1 + \frac{1}{2} \sin^2(\theta) \right) \left[S_2^{(p)}(\mathbf{r}) - \phi_p^2 \right] \\ & + \frac{2ik_q^3}{3} \frac{3}{4\pi} \int d\mathbf{r} \left[S_2^{(p)}(\mathbf{r}) - \phi_p^2 \right] \end{aligned} \quad (\text{C3})$$

and

$$\begin{aligned} V = & \frac{3}{4\pi} \int \frac{d\mathbf{r}}{r^3} (-1 + 3 \cos^2(\theta)) (S_2^{(p)}(\mathbf{r}) - \phi_p^2) + \frac{k_q^2}{2} \frac{3}{4\pi} \int \frac{d\mathbf{r}}{r} (1 + \cos^2(\theta)) \left[S_2^{(p)}(\mathbf{r}) - \phi_p^2 \right] \\ & + \frac{2ik_q^3}{3} \frac{3}{4\pi} \int d\mathbf{r} \left[S_2^{(p)}(\mathbf{r}) - \phi_p^2 \right], \end{aligned} \quad (\text{C4})$$

where we have used the fact that the two in-plane matrix components must be equal in order to simplify the integrals.

In Ref. 36, the first integral in the expression for V was evaluated analytically for the case of hard oriented spheroids. In what follows, we specialize to this model. We evaluate the first two integrals in each of the relations (C3) and (C4) numerically. Note that the

third integral in each expression, which we denote by U_3 and V_3 , respectively, are identical, and may be obtained analytically as follows:

$$\begin{aligned}
U_3 = V_3 &= \frac{2ik_q^3}{3} \frac{3}{4\pi} \int d\mathbf{r} \left[S_{2,HS}^{(p)}(\mathbf{r}; b/a) - \phi_p^2 \right] \\
&= \frac{4\pi ik_q^3}{3} \frac{3}{4\pi} \int_{-1}^1 d\cos(\theta) \int_0^\infty dr r^2 \left[S_{2,HS}^{(p)}(\sigma_0(r/\sigma(\theta)); 1) - \phi_p^2 \right] \\
&= ik_q^3 \int_{-1}^1 d\cos(\theta) \int_0^\infty dr r^2 \left[S_{2,HS}^{(p)}(\sigma_0(r/\sigma(\theta)); 1) - \phi_p^2 \right] \\
&= ik_q^3 \int_{-1}^1 d\cos(\theta) \left[\frac{\sigma(\theta)}{\sigma_0} \right]^3 \int_0^\infty dr r^2 \left[S_{2,HS}^{(p)}(r; 1) - \phi_p^2 \right] \\
&= 2ik_q^3 \frac{b}{a} \int_0^\infty dr r^2 \left[S_{2,HS}^{(p)}(r; 1) - \phi_p^2 \right], \tag{C5}
\end{aligned}$$

where we have used the mapping between the two-point function $S_{2,HS}^{(p)}(\mathbf{r}; b/a)$ for the hard-spheroid model and $S_{2,HS}^{(p)}(\mathbf{r}; 1)$ for the corresponding hard-sphere system described in Section III.C. Note that the radial integral in the last line of (C5) is proportional to the zero-wave-vector of the structure factor of the hard-sphere system. For an equilibrium distribution, this may be obtained analytically directly from the Percus-Yevick approximation, for example. The two-point approximation to the dielectric tensor is obtained by truncating the series expansion given in Eq. (19) after the second term to yield

$$\beta_{pq}^2 \phi_p^2 (\varepsilon_e - \varepsilon_q \mathbf{I})^{-1} (\varepsilon_e + 2\varepsilon_q \mathbf{I}) = \phi_p \beta_{pq} \mathbf{I} - \mathbf{A}_2^{(p)} \beta_{pq}^n. \tag{C6}$$

-
- [1] J. C. Maxwell, *A Treatise on Electricity and Magnetism* (Clarendon Press, Oxford, 1873).
 - [2] L. Tsang, J. A. Kong, and R. Shin, *Theory of Microwave Remote Sensing* (Wiley, New York, 1985).
 - [3] V. I. Tatarskii, *The Effects of the Turbulent Atmosphere on Wave Propagation* (Jerusalem: Israel Program for Scientific Translations, 1971).
 - [4] C. Meola, G. M. Carlomagno, A. Squillace, and G. Giorleo, *Measurement Sci. Tech.* **13**, 1583 (2002).
 - [5] N. P. Zhuck, *Phys. Rev. B* **50**, 15636 (1994).
 - [6] R. C. McPhedran and D. R. McKenzie, *Appl. Phys. A* **23**, 223 (1980)
 - [7] A. Mejdoubi and C. Brosseau, *J. Appl. Phys.* **101**, 084109 (2007).

- [8] T. I. Zohdi, *Comput. Methods Appl. Mech. Engrg.* **195**, 5813 (2006).
- [9] R. C. McPhedran, L. C. Botten, A. A. Asatryan, N. A. Nicorovici, P. A. Robinson, and C. M. de Sterke, *Phys. Rev. E* **60**, 7614 (1999).
- [10] P. Sheng, *Introduction to Wave Scattering, Localization and Mesoscopic Phenomena* (Springer-Verlag, New York, 2006).
- [11] L. Tsang and J. A. Kong, *Rad. Sci.* **16**, 303 (1981).
- [12] D. Klusch, Th. Pflug, and K. O. Thielheim, *Phys. Rev. B* **47**, 8539 (1993).
- [13] T. G. Mackay, A. Lakhtakia, and W. S. Weiglhofer, *Phys. Rev. E* **64**, 66616 (2001).
- [14] M. Beran, *Statistical Continuum Theories* (Wiley, New York, 1968).
- [15] G. W. Milton, *Phys. Rev. Lett.* **46**, 542 (1981).
- [16] R. C. McPhedran and G. W. Milton, *Appl. Phys. A* **26**, 207 (1981).
- [17] S. Torquato, *J. Appl. Phys.* **58**, 3790 (1985); A. Sen and S. Torquato, *Phys. Rev. B* **39**, 4504 (1989).
- [18] S. Torquato and F. Lado, *Phys. Rev. B* **33**, 6428 (1986).
- [19] S. Torquato, *Random Heterogeneous Materials: Microstructure and Macroscopic Properties* (Springer, 2002).
- [20] S. Torquato and G. Stell, *J. Chem. Phys.* **77**, 2071 (1982).
- [21] R. H. J. Kop, P. de Vries, R. Sprik, and A. Lagendijk, *Phys. Rev. Lett.* **79**, 4369 (1997).
- [22] Z. Q. Zhang, I. P. Jones, H. P. Schriemer, J. H. Page, D. A. Weitz, and P. Sheng, *Phys. Rev. E* **60**, 4843 (1999).
- [23] B. Lu and S. Torquato, *J. Opt. Soc. Am* pp. 717 (1990).
- [24] S. Torquato and F. H. Stillinger, *Phys. Rev. E* **68**, 41113 (2003).
- [25] Note that there exist hyperuniform systems that are disordered, (e.g., maximally random jammed sphere packings), and therefore, $C_\infty = 0$ does not necessarily imply the absence of disorder (see Refs. 24, 41).
- [26] D. J. Eyre and G. W. Milton, *Eur. Phys. J. Ap.* **6**, 41 (1999).
- [27] D. C. Pham and S. Torquato, *J. Appl. Phys.* **94**, 6591 (2003).
- [28] Z. Hashin and S. Shtrikman, *J. Appl. Phys.* **33**, 3125 (1962).
- [29] J. R. Willis, *J. Mech. Phys. Solids* **25**, 185 (1977).
- [30] S. Torquato, *Ind. Eng. Chem. Res.* **45**, 6923 (2006).
- [31] P. Debye, H. R. Anderson Jr, and H. Brumberger, *J. Appl. Phys.* **28**, 679 (2004).

- [32] C. L. Y. Yeong and S. Torquato, Phys. Rev. E **57**, 495 (1998).
- [33] Y. Jiao, F. H. Stillinger, and S. Torquato, in preparation (2007).
- [34] J-P. Hansen and I. R. McDonald, *Theory of Simple Liquids* (Academic Press, New York, 2006).
- [35] S. Torquato and G. Stell, J. Chem. Phys. **82**, 980 (1985).
- [36] S. Torquato and F. Lado, J. Chem. Phys. **94**, 4453 (1991).
- [37] M. D. Rintoul and S. Torquato, J. Phys. A: Math. Gen **30**, L585 (1997).
- [38] M. J. D. Powell, Mol. Phys. **7**, 591 (1964).
- [39] S. Torquato, Phys. Rev. Lett. **79**, 681 (1997); S. Torquato, J. Mech. Phys. Solids **45**, 1421 (1997); S. Torquato, J. Mech. Phys. Solids **46**, 1411 (1998).
- [40] D. Levine and P. J. Steinhardt, Phys. Rev. Lett. **53**, 2477 (1984).
- [41] A. Donev, F. H. Stillinger, and S. Torquato, Phys. Rev. Lett. **95**, 90604 (2005).